Hiroshima University Doctoral Thesis

Photochemical [2+2] Cycloaddition Reaction of Carbonyl Compounds with Danishefsky-Kitahara Diene

(Danishefsky-Kitahara ジエンとカルボニル化合物との光[2+2]付加環化反応)

2020

Department of Chemistry,

Graduate School of Science,

Hiroshima University

Dian Agung Pangaribowo

# Table of Contents

Main Thesis

Contents

Chapter 1

General Introduction

1.1 Electronically excited states in organic reactions

The field of organic photochemistry has been started in 1900 when Ciamician and Silber exposed a solution of benzophenone in isopropanol to sunlight.[1] They described the product as a condensation of benzophenone with acetaldehyde. This condition was happened because of the inaccurate combustion analysis and a lack of chemical degradation studies. Then, Ciamician has tried to recalling his own previous work on photoreduction-oxidation reactions and repeated this study. He found the structure of the irradiation product as benzopinacol. Although Ciamician and Silber did not utilize the photoreaction as a useful and widely applied photochemical reaction, they are generally given the credit because they discovered the structure of the photodimer.[2]

The mechanism of benzophenone transformation[3–5] (Scheme 1) involves the formation of the singlet excited state of benzophenone, followed by the intersystem crossing to the triplet excited state of benzophenone. The triplet species, which has a radical characteristic, abstracts a hydrogen atom from the isopropyl alcohol to generate the radical. A coupling of the radical gives the benzopinacol photoproduct.

Scheme 1 Mechanism of the transformation of benzophenone to benzopinacol
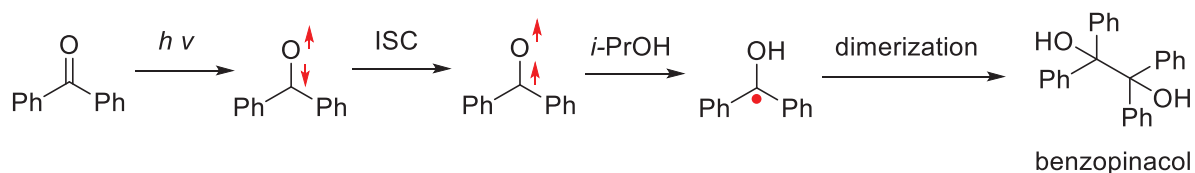
According to quantum theory, light is also quantized. The absorption or emission of light occurs by the transfer of energy as photons. These photons have both wavelike and particle-like properties, and each photon has a specific energy. In the absorption of light, a photon can use its energy to move an electron from the lower energy level to the upper one, producing an electronically-excited state. The production of the electronically-excited state by photon absorption is the aspect that defines photochemistry and separates it from other branches of chemistry.

When a singlet-state molecule in a ground-state (S_0) absorbs light, the electron can reach an electronically excited state with opposite spins, which called singlet excited state (S_1) (Scheme 2). Then the excited state crosses to the triplet excited state (T_1), which the two-electrons have parallel spins, via the intersystem crossing (ISC) process.

Scheme 2 Molecular orbital diagram showing the orbital and their occupancy in the ground-state (S_0), singlet excited state (S_0), and in an triplet excited state (T_1)
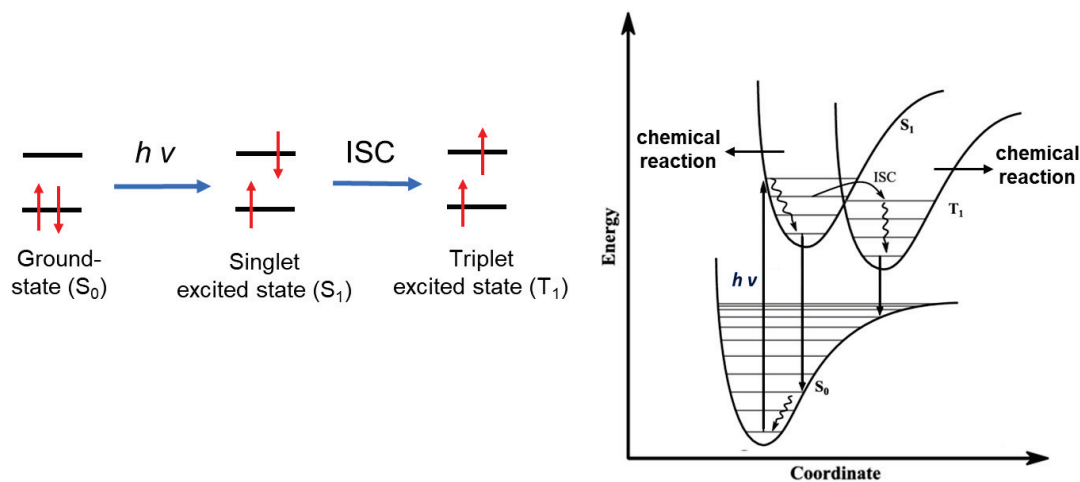
Irradiation of a molecule in suitable energy will induce photochemical reactions. The chemoselectivity, regioselectivity, and stereoselectivity of photochemical reactions significantly differ from those of thermal reactions. Photochemical reactions are the reactions of excited-state molecules, which begin by photon absorption, whereas thermal reactions are the reactions of ground-state molecules, which usually triggered by heat. Excited-state molecules are more reactive than the corresponding ground-state molecules, resulted in a higher number of possible reactions available from the excited state than from the ground state. Typical examples of photoreactions, which should not be achieved in the ground-state, are [2+2] photocycloaddition reaction, photoisomerization reaction, and hydrogen abstraction reaction.

a. [2+2] photocycloaddition reaction

According to the Woodward–Hoffmann rule, the [2+2] cycloaddition reaction between two alkenes is photochemically symmetry-allowed, but it is symmetry-forbidden at the ground state.[6] A cycloaddition reaction between two alkene molecules produces a cyclobutane ring by establishing two new σ-bonds (Scheme 3). The direct photoreaction involves the concerted reaction of the singlet $^1(\pi, \pi^*)$ excited state of one alkene with the ground state of the other.

2

Scheme 3 The [2+2] photocycloaddition reaction between two alkenes produces cyclobutene ring
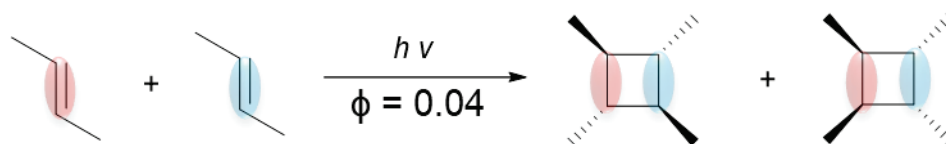
The triplet sensitization is a very efficient way of promoting photocycloaddition of quite rigid alkenes. The sensitizer is necessary because alkenes generally do not go through efficient intersystem crossing from the singlet state generated by direct excitation. By this method, the photocycloaddition of cyclopentene gives tricyclic dimers (Scheme 4).[7]

Scheme 4 The [2+2] photocycloaddition reaction of cyclopentene produces tricyclic dimers
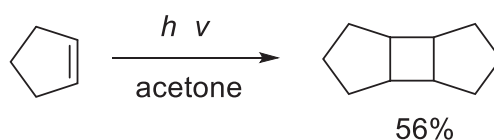
b. Photoisomerization reaction

The switch of geometrical isomers of alkenes using thermal or catalytic methods generates a thermodynamic equilibrium mixture of isomers. For example, the *cis* isomer of stilbene reacts to produce mainly the more stable *trans* isomer when heated strongly. The photochemical isomerization involves an excited state of the alkene, and it gives a route to the thermodynamically less stable isomer. When either the *cis* or the *trans* isomer of an alkene is irradiated, a mixture of both isomers will be found in a particular ratio. This ratio is called the photostationary state composition. For the *trans*-stilbene, by using a 313 nm light source, it will give a photostationary state mixture containing 93% *cis*-stilbene (Scheme 5).[8]

Scheme 5 The photoisomerization of stilbene
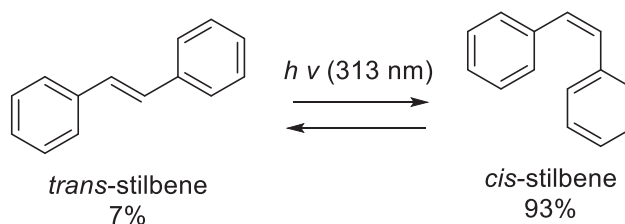
Photochemical isomerization of alkenes can also take place through triplet states. Triplet–triplet energy transfer allows the efficient indirect production of triplet molecules, which are not accomplished of being produced directly due to inefficient intersystem crossing (Scheme 6). For triplet-triplet energy transfer to occur, the lowest triplet state of the donor must be higher in energy than the lowest triplet state of the acceptor. Since ketones have a small singlet-triplet energy gap, this compound is suitable to act as a photosensitizer. Their high triplet quantum yields make them excellent triplet photosensitizers.

Scheme 6 Photosensitised isomerization of alkenes
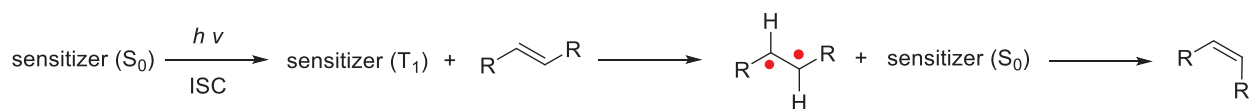
The photochemistry of the eyesight process is an example of an isomerization reaction in the biological system. After the 11-*cis*-retinal absorbs a photon, it will undergo photoisomerization into its isomer all-*trans*-retinal (Figure 1).[9] Because of this photoisomerization; structural changes arise within the confines of the binding cavity, which in turn produce changes to the cell membrane and generate a signal that is sent to the brain.

(a)   **(b)**
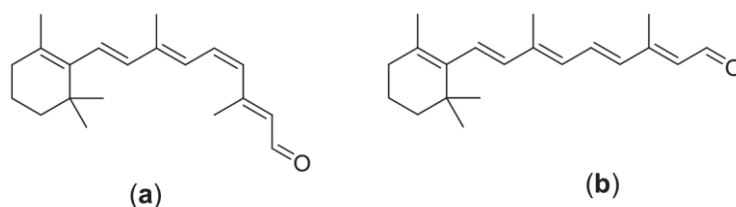
Figure 1 11-*cis*-retinal (a); and all-*trans*-retinal

c. Hydrogen abstraction reaction

One of the principal reaction types for ketone excited states is hydrogen abstraction (Scheme 7). In each case, the weakest C-H bond in the R-H molecule is broken. The pair of radicals that are initially generated can react in several ways, which are combined with each other, dimerize or abstract a second hydrogen atom.

Scheme 7 Abstraction of hydrogen by excited-state benzophenone

4
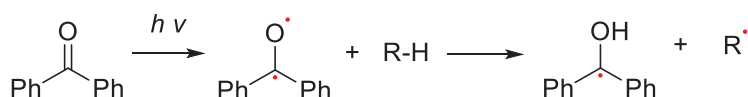
Hydrogen abstraction can also occur from a γ-position within the ketone molecule to generate a diradical that may cyclize (Yang cyclization) by a combination of the radical centers to the four-membered cyclic alcohol (Scheme 8). Alternatively, the bond cleavage of the C–C bond in the diradical can occur to form an alkene and an enol. The enol rapidly isomerizes to a ketone with fewer carbon atoms than the parent ketone. The reaction is known as a photo elimination reaction, commonly referred to as the Norrish type 2 reaction.

Scheme 8 Intramolecular hydrogen abstraction reaction
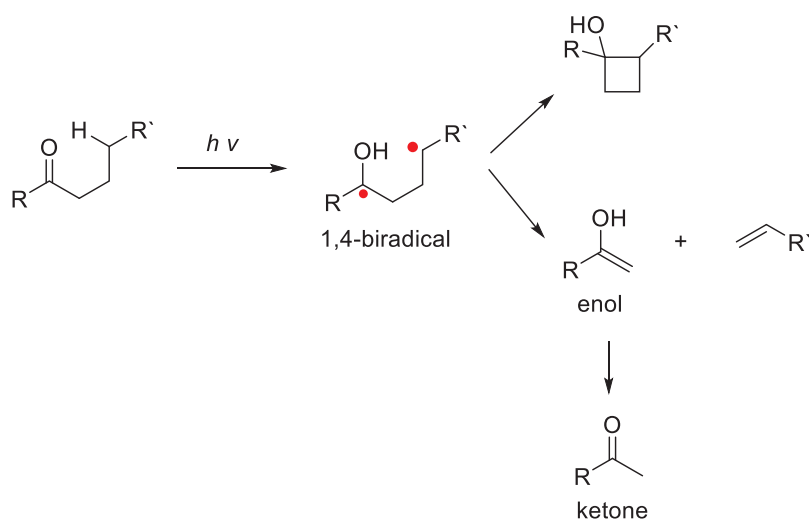
Photochemical reactions occur all around us, being an essential aspect of many of the chemical processes occurring in living systems and in the environment. The capability and versatility of photochemistry are increasingly becoming important in improving the quality of our lives through health care, energy production, and the search for solutions to some of the problems of the modernized world. Many industrial and technological processes depend on applications of photochemistry. The development of many new devices has been made possible by the result of photochemical research.[10] New products that are challenging in the synthesis using ground-state reactions are thus available[11] (Scheme 9), opening new perspectives in search of biologically active compounds.[12]

Scheme 9 Synthesis of 3,3-Diphenyloxetane using photochemical reaction
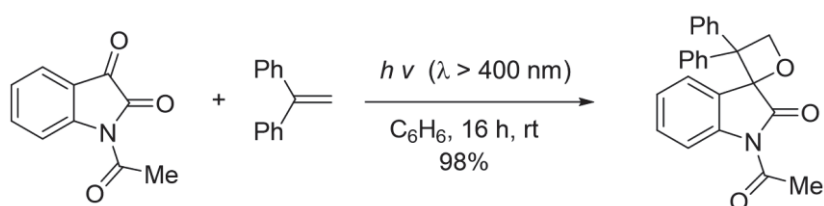
1.2 Oxetanes: properties and synthesis

Oxetanes, which is four-membered cyclic ethers, have a ring strain energy of approximately 110 kJ mol^{-1} [13] and polar properties of the C-O bonds. These features make them attractive motifs for applications in chemical science. Recent interest in this heterocycle is partly due to its biological activity. Oxetane rings have gained significant attention in medicinal chemistry as they can replace the gem-dimethyl and carbonyl groups to increase the "druglike" properties of a compound, especially its water solubility.[14] Several biologically active oxetane-containing compounds have been found in nature (Figure 2), including the taxol derivative 7-epi-10-deacetyltaxol with anticancer activity,[15] norfriedelin A with acetylcholinesterase inhibitor activity,[16] and macrolactins with antimicrobial activity.[17] Other naturally occurring oxetane-containing compounds such as ebelactone B and belactins A & B are found to be potent inhibitors of pancreatic lipase[18] and serine carboxypeptidase,[19,20] respectively.
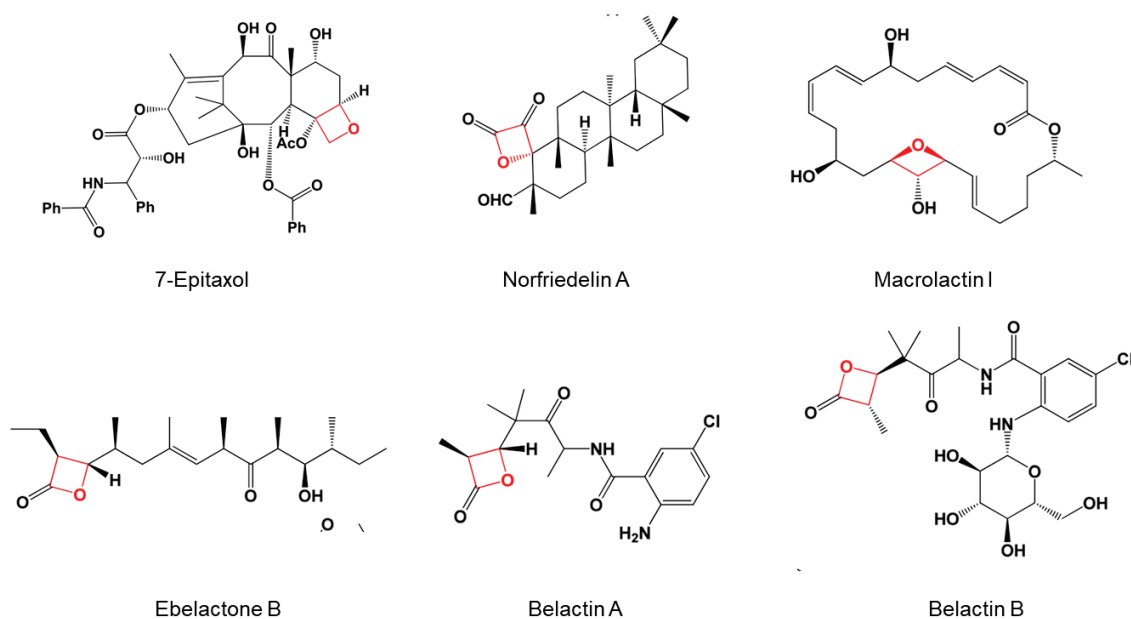
Figure 2 Biologically active compounds containing oxetane rings

Recent studies have relied on synthetic methods and the development of new methodologies for oxetane synthesis and incorporation. Accordingly, several novel approaches have been developed to access oxetane-containing compounds. At the same time, there have been significant advances in utilizing the reactivity of oxetanes in the synthesis of complex molecules. The ring strain in oxetane makes the cyclization process become a fundamental synthetic challenge. The kinetics of cyclization to form four-membered saturated cyclic ethers are significantly slower than for three-, five-, and six-membered analogues.[21] Therefore, anions

and good leaving groups are commonly required to achieve the cyclization of acyclic precursors to oxetane derivatives. The most common disconnection forms the C−O bond through an intramolecular etherification reaction, which has been produced by several approaches (i.e., Williamson-type reaction), complemented by C−C bond-forming methods (i.e., the ring-expansion reaction of epoxides).

Williamson-type etherification reaction describes a general approach to ether synthesis. This reaction is a base-mediated nucleophilic substitution reaction between an alcohol and an aliphatic carbon center in a 1,3-relationship for oxetane synthesis. Furthermore, the intramolecular cyclization generally provides the desired oxetane products. This approach was first used for the synthesis of oxetane in 1878 by Reboul[22]. Later, this method was employed in the synthesis of complex oxetane-containing structures[23] (Scheme 10A). However, the chemical yields can be decreased due to undesirable side reactions, such as fragmentation of the halo-alkoxide into an aldehyde and an alkene[24] (Scheme 10B). Consequently, intramolecular Williamson etherification is rather substrate-dependent.

Scheme 10 Intramolecular Williamson etherification (A) formation of oxetanes (B) fragmentation side reaction

(A)

(B)
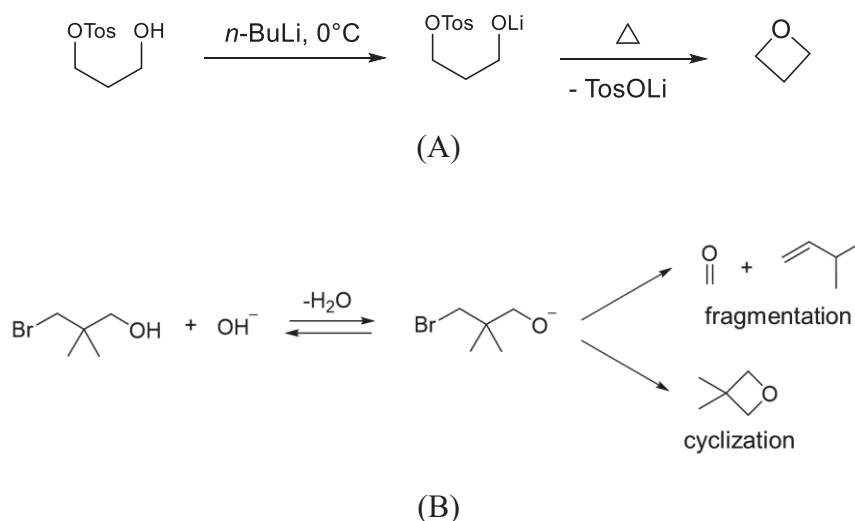
As an alternative of the Williamson etherification, epoxides can undergo ring-expansion to form oxetanes. The cyclization precursor can be constructed by opening an epoxide with nucleophiles bearing leaving groups. In 1983, Okuma *et al.*[25] reported a method to access the oxetane by ring-opening of epoxides with trimethyloxosulfonium iodide, which will produce a sulfoxonium ylide. Then the cyclization occurred in the same reaction flask with the release of dimethyl sulfoxide to afford 2-substituted oxetanes in excellent yields of 83−99% (Scheme 11).

However, this method is limited to produce less-substituted oxetanes

Scheme 11 The formation of oxetanes by ring-expansion reactions
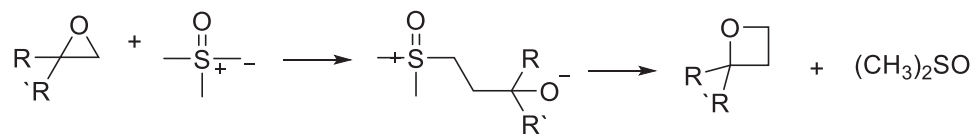
1.3 Paternò–Büchi reaction

The photochemical [2+2] cycloaddition reaction of alkenes with carbonyl compounds, referred to as the Paternò–Büchi (PB) reaction, was first reported in 1909[26,27] and is currently one of the versatile methods for oxetane synthesis. The product distribution and reaction mechanism of the PB reaction, especially with furan derivatives, which are cyclic s-*cis* dienes, have been extensively studied.[12,28–34] In the ground state of the carbonyl (C=O) group, the oxygen atom has a nucleophilic character, while the carbon atom has an electrophilic character. The nπ* electronic excitation of the carbonyl group imparts umpolung character to the carbonyl group.[35] In general, the intersystem crossing from the singlet to the triplet state is rapid enough to generate the triplet excited state of aromatic carbonyls. The long-lived triplet excited state of carbonyls can react intermolecularly with an alkene to produce intermediary triplet 1,4-diradicals 1,4-**DR** or radical ion pairs RI. In the case of aliphatic carbonyls, the singlet excited state can react with alkenes to obtain singlet 1,4-diradicals directly (Scheme 12). The radical ion RI is formed if the photoinduced electron transfer (PET) reaction is energetically favorable. However, if the PET reactions are energetically unfavorable, the formation of 1,4-diradicals 1,4-**DR** becomes essential for oxetane formation.

Scheme 12 The generally accepted mechanism of the PB reaction
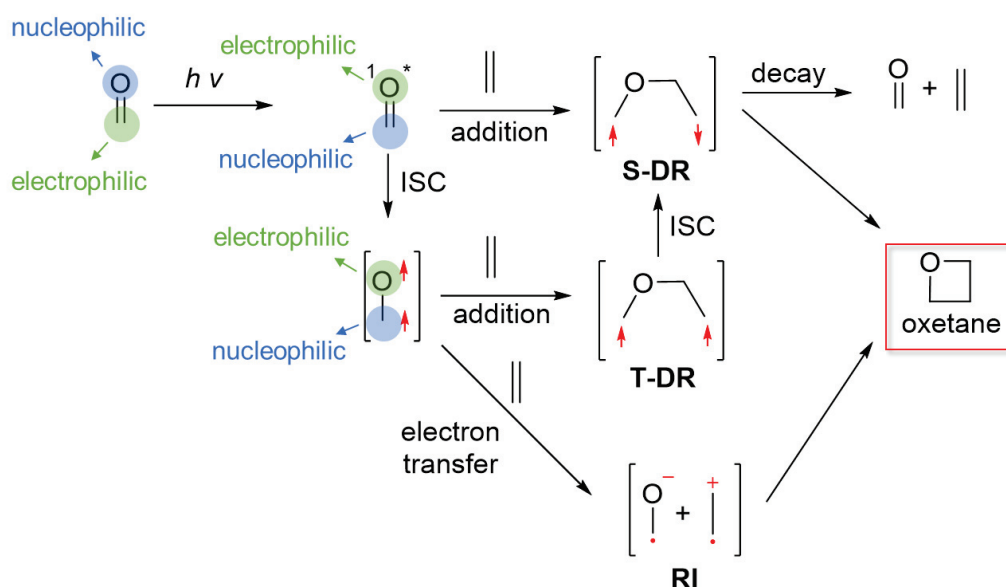
The singlet 1,4-diradical intermediate, **S-DR**, has two possible paths, which is bond formation to give the oxetane, or bond cleavage to give the starting materials. Thus, the ratio between oxetane formation and bond cleavage plays a vital role in the determination of

regioselectivity, site-selectivity, and stereoselectivity during oxetane formation.[36]

The regioselectivity of the oxetane formation can be explained by the diradical-stability rule (Scheme 13). The intermediary diradical **DR1** is supposed to be more stable than the diradical **DR2**. When the nucleophilicities of the two carbons in alkenes differ significantly, regioselectivity can be explained by the difference in the HOMO coefficient. Thus, in a furan ring, the C-2 carbon is known to be more nucleophilic compare to C-3 (Scheme 14).

Scheme 13 Regioselectivity of oxetane formation based on the radical stability rule
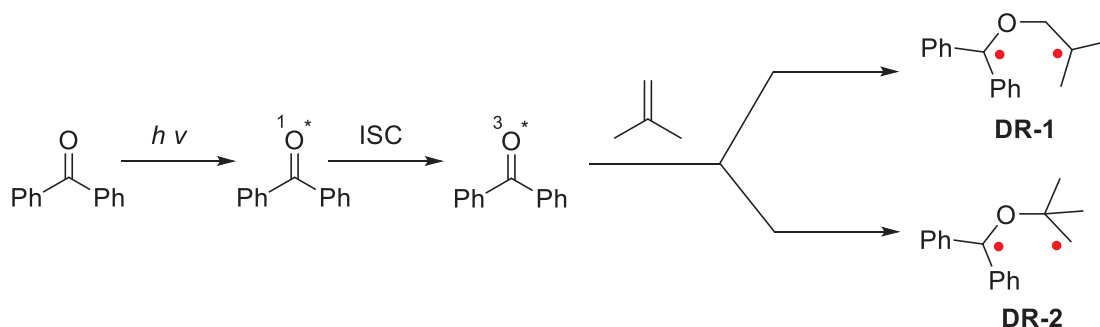
Scheme 14 Regioselectivity of oxetane formation based on nucleophilicity rule
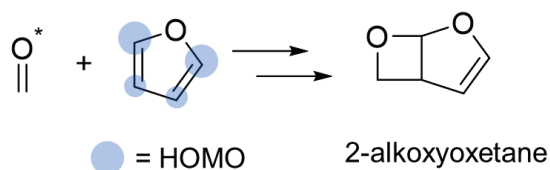
When the electron transfer mechanism between electron-rich alkenes and excited carbonyl compounds is energetically favorable, the RI pair becomes a crucial intermediate in photochemical [2+2] cycloaddition reactions (Scheme 12). The regioselectivity of these mechanisms may differ from that involving the formation of 1,4-triplet diradical intermediates. Typical examples of PB reactions with very electron-rich alkenes, ketene silyl acetals (KSA) (E_{ox} = 0.9 V vs SCE), have been reported (Scheme 15).[37] The photoreactions of aromatic ketones with electron-rich KSA afforded the regioselective formation of 2-siloxyoxetane. The regioselectivity has been explained by the electron transfer oxidation of KSA, provided the spin of the KSA radical cation is localized at the β-carbon. Besides the exclusive formation of 2-alkoxy-oxetanes in the photoreaction of 2-naphthaldehyde with KSA, the silyl-migration adduct was also found. The product ratios between 2-alkoxyoxetane and silyl-migration adduct were mostly dependent on the solvent used and the silyl group. In non-polar solvents, regioselective formation occurs to give the 2-alkoxyoxetanes via 1,4 diradical 1,4-DR. In polar

solvents, the formation of the 2-alkoxyoxetane can compete with the formation of the silyl-migration adduct. When the silyl group is considerably bulky (such as TES and TBDMS), the solvation of the cationic silicon atom is suppressed to give the 2-alkoxyoxetane.

Scheme 15 The photoreaction of 2-naphthaldehyde with KSA
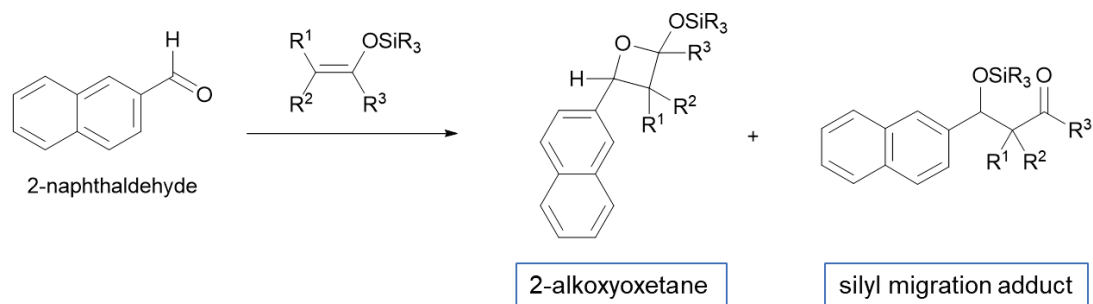
1.4 References

1   G. Ciamician and P. Silber, *Chem. Ber.*, 1900, **33**, 2911.

2   N. D. Heindel and M. A. Pfau, *J. Chem. Educ.*, 1965, **42**, 383–386.

3   J. N. Pitts, R. L. Letsinger, R. P. Taylor, J. M. Patterson, G. Recktenwald and R. B. Martin, *J. Am. Chem. Soc.*, 1959, **81**, 1068–1077.

4   W. M. Moore, G. S. Hammond and R. P. Foss, *J. Am. Chem. Soc.*, 1961, **83**, 2789–2794.

5   J. A. Bell and H. Linschitz, *J. Am. Chem. Soc.*, 1963, **85**, 528–533.

6   P. G. Bauslaugh, *Synthesis (Stuttg).*, 1970, **1970**, 287–300.

7   R. G. Salomon, K. Folting, W. E. Streib and J. K. Kochi, *J. Am. Chem. Soc.*, 1974, **96**, 1145–1152.

8   C. R. Crecca and A. E. Roitberg, *J. Phys. Chem. A*, 2006, **110**, 8188–8203.

9   P. S. Bernstein, W. C. Law and R. R. Rando, *Proc. Natl. Acad. Sci. USA*, 1987, **84**, 1849–1853.

10   B. Wardle, *Principles and Applications of Photochemistry*, John Wiley & Sons Ltd, Manchester, 2009.

11   J. Xue, Y. Zhang, T. Wu, H. K. Fun and J. H. Xu, *J. Chem. Soc. Perkin Trans. 1*, 2001, 183−191.

12   N. Hoffmann, *Chem. Rev.*, 2008, **108**, 1052.

13   B. Ringnér, S. Sunner and H. Watanabe, *Acta Chem. Scand.*, 1971, **25**, 141–146.

14   J. A. Bull, R. A. Croft, O. A. Davis, R. Doran and K. F. Morgan, *Chem. Rev.*, 2016, **116**, 12150–12233.

15   K. Subban, S. Singh, R. Subramani, M. Johnpaul and J. Chelliah, *BMC Complement. Altern. Med.*, 2017, **17**, 1–16.

16   J. Q. Liu, X. R. Peng, X. Y. Li, T. Z. Li, W. M. Zhang, L. Shi, J. Han and M. H. Qiu, *Org. Lett.*, 2013, **15**, 1580–1583.

17   M. A. M. Mondol, F. S. Tareq, J. H. Kim, M. A. Lee, H. S. Lee, Y. J. Lee, J. S. Lee and H. J. Shin, *J. Nat. Prod.*, 2011, **74**, 2582–2587.

18   H. Ostrowska, J. Kalinowska, E. Chabielska, A. Stankiewicz, K. Kruszewski and W. Buczko, *J. Cardiovasc. Pharmacol.*, 2005, **45**, 348–353.

19   S. Murakami, S. Harada, F. Kojima, N. Kinoshita, Y. Takahashi, M. Hamada, T. Takeuchi and T. Aoyagi, *J. Enzyme Inhib. Med. Chem.*, 1995, **9**, 263–275.

20   S. Murakami, Y. Takahashi, H. Naganawa, T. Takeuchi and T. Aoyagl, *J. Enzyme Inhib. Med. Chem.*, 1995, **9**, 277–284.

21   A. Di Martino, C. Galli, P. Gargano and L. Mandolini, *J. Chem. Soc. Perkin Trans. II,*

1985, 1345–1349.

22 M. Reboul, *Ann. Chim.*, 1878, **14**, 495−497.

23 P. Picard, D. Leclercq, J. P. Bats and J. Moulines, *Synthesis (Stuttg).*, 1981, **1981**, 550–551.

24 S. Searles, R. G. Nickerson and W. K. Witsiepe, *J. Org. Chem.*, 1959, **24**, 1839–1844.

25 K. Okuma, Y. Tanaka, S. Kaji and H. Ohta, *J. Org. Chem.*, 1983, **48**, 5133–5134.

26 E. Paternó and G. Chieffi, *Gazz. Chim. Ital.*, 1909, **39**, 341–361.

27 G. Büchi, C. G. Inman and E. S. Lipinsky, *J. Am. Chem. Soc.*, 1954, **76**, 4327–4331.

28 A. G. Griesbeck and S. Stadtmüller, *J. Am. Chem. Soc.*, 1991, **113**, 6923.

29 A. G. Griesbeck, H. Mauder and S. Stadtmuller, *Acc. Chem. Res.*, 1994, **27**, 70.

30 M. Abe, E. Torii and M. Nojima, *J. Org. Chem.*, 2000, **65**, 3426–3431.

31 M. D'Auria, R. Racioppi and G. Romaniello, *European J. Org. Chem.*, 2000, **2000**, 3265–3272.

32 M. Abe, T. Kawakami, S. Ohata, K. Nozaki and M. Nojima, *J. Am. Chem. Soc.*, 2004, **126**, 2838–2846.

33 M. Abe, M. Terazawa, K. Nozaki, A. Masuyama and T. Hayashi, *Tetrahedron Lett.*, 2006, **47**, 2527–2530.

34 Y. Yabuno, Y. Hiraga, R. Takagi and M. Abe, *J. Am. Chem. Soc.*, 2011, **133**, 2592–2604.

35 M. Abe, in *Handbook of Synthetic Photochemistry*, eds. Angelo Albini and Maurizio Fagnoni, Wiley-VCH, Weinheim, 2010, pp. 217–239.

36 H. Buschmann, H.-D. Scharf, N. Hoffmann and P. Esser, *Angew. Chem. Int. Ed. Engl.*, 1991, **30**, 477–515.

37 M. Abe, Y. Shirodai and M. Nojima, *J. Chem. Soc. - Perkin Trans. 1*, 1998, 3253–3260.

Chapter 2

Photochemical [2+2] Cycloaddition Reaction of Carbonyl Compounds with Danishefsky-Kitahara Diene

2.1 Introduction

        Danishefsky and Kitahara developed an acyclic siloxydiene, *trans*-1-methoxy-3-trimethylsilyloxy-buta-1,3-diene (*trans*-**1**). It is also known as the Danishefsky-Kitahara diene and is a useful reagent in organic synthesis.[1] Since the diene is an electron-rich nucleophile, it proved to be a powerful reagent in the Mukaiyama aldol addition and Diels-Alder reactions. For example, the reaction of benzaldehyde (**2a**) with *trans*-**1** at −78 °C in propionitrile solvent in the presence of 20 mol% acid catalyst afforded mainly the Mukaiyama aldol product **3** (Scheme 1).[2] The C1 carbon of *trans*-**1** is the most nucleophilic center, and thus, reacts with the electrophilic carbonyl carbon of **2a** to give the final 1,3 ketol product **3**. The hetero Diels-Alder reaction of **2a** with *trans*-**1** using a chiral zirconium catalyst[3] gave the pyranone product **4** in 35% yield and 62% ee selectivity (Scheme 2).[4]

Scheme 1 Mukaiyama aldol addition reaction of Danishefsky-Kitahara diene with benzaldehyde
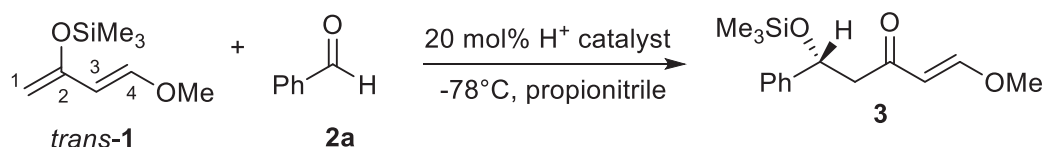
Scheme 2 Hetero Diels Alder reaction of Danishefsky-Kitahara diene with benzaldehyde
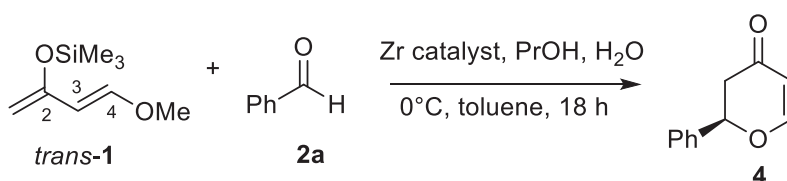
        Several studies on the PB reaction of silyl enol ethers have been reported. For example, the photoreactions of aromatic ketones with electron-rich ketene silyl acetals (KSA) afforded the regioselective formation of 2-siloxyoxetane.[5] The contrast results on the regioselectivity in the formation of siloxyoxetanes was found on PB reaction of silyl O,S-ketene acetals (SKA), and aromatic aldehydes (scheme 3).[6] The photoreaction of aldehydes with SKA has been found to give *trans*-3-siloxyoxetanes independent upon the aldehyde, the substituents SR^1 and SiR_3, and solvent. The triplet 2-oxatetramethylene 1,4-diradical T-1,4-DR is proposed as an intermediate.

Scheme 3 The photoreaction of benzaldehyde with SKA
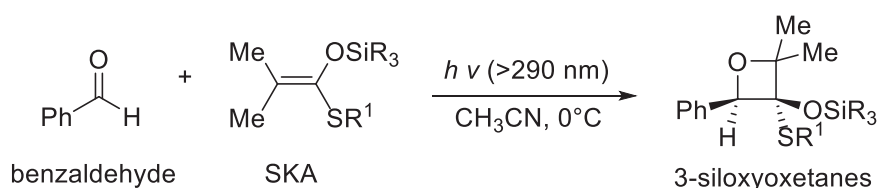
benzaldehyde   SKA   3-siloxyoxetanes

So far, the PB reaction of acyclic conjugated dienes has not been studied. This is because the dienes are well-known to physically, rather than chemically, quench the triplet state of ketones, owing to their low triplet energy, E_T (~ 55 kcal mol^{-1}). In this chapter, the PB reaction of *trans*-**1** with benzophenone (**2b**) was examined for the first time, in which the formation of oxetanes **5** and **7** were found in high yields.[7] The photochemically activated carbonyl compound reacted with *trans*-**1** to produce the C–C coupling compounds coupled at C2 and C3 carbon atoms, rather than C1 carbon atom. The chemoselectivities of the former are different from the Lewis acid-promoted reaction, indicating the synthetic utility of excited state (Scheme 4).

Scheme 4 Mukaiyama aldol addition reaction, hetero Diels Alder reaction, and photochemical PB reaction of Danishefsky-Kitahara diene with carbonyl compounds

15
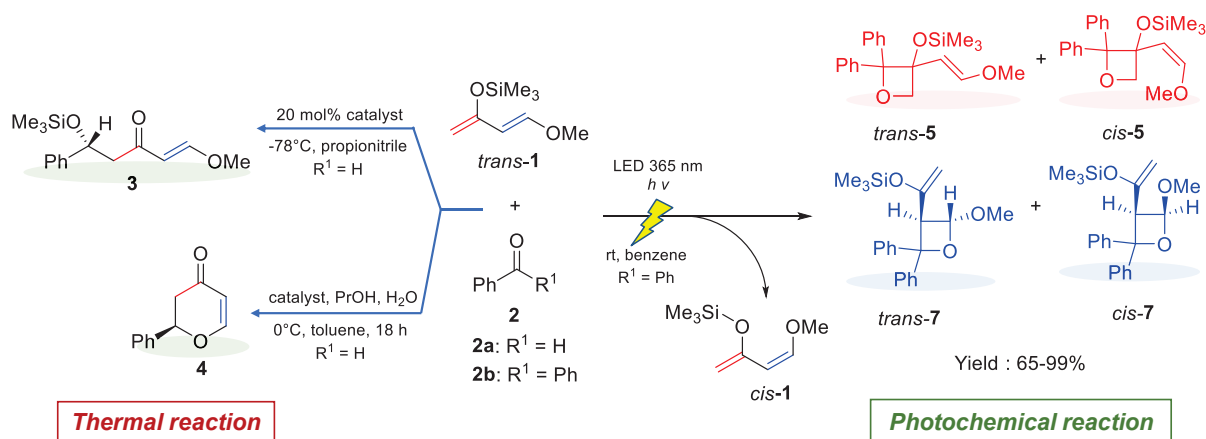
2.2 Results and discussion

A degassed benzene solution of **2b** (0.2 M, Figure 1b) and *trans*-**1** (0.6 M, Figure 1a) was irradiated with a 365 nm LED lamp at room temperature in a sealed nuclear magnetic resonance (NMR) tube. The reaction progress was directly monitored by ^{1}H NMR measurements (Figures. 1c-f). After 1 h of irradiation (Figure 1d, Figure 2), new signals at δ 0.2, 3.0, 4.6, 4.7, 5.1, and 5.6 ppm were observed, in addition to the signals existing before irradiation (Figure 1c). The new signals were identified to be those from *cis*-**1**, which is an isomer of *trans*-**1**.
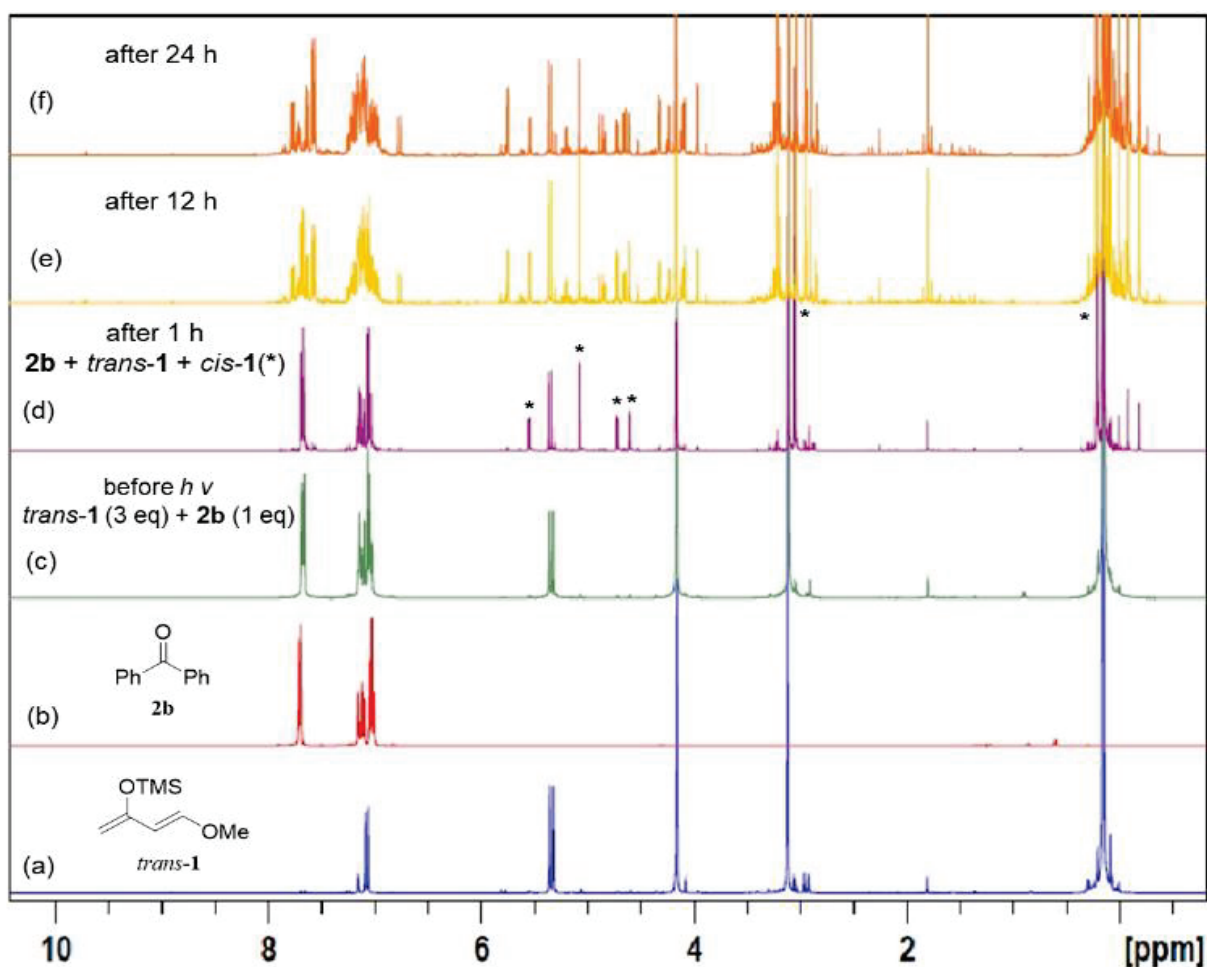
Figure 1 ^{1}H NMR (400 MHz, C$_6$D$_6$) spectroscopic analysis of the photochemical reaction of *trans*-**1** with **2b** under irradiation at 365 nm. (a) *trans*-**1**, (b) **2b**, (c) before irradiation at 20°C, (d) after 1 hour irradiation at 365 nm, (e) after 12 hour irradiation at 365 nm, and (f) after 24 hour irradiation at 365 nm
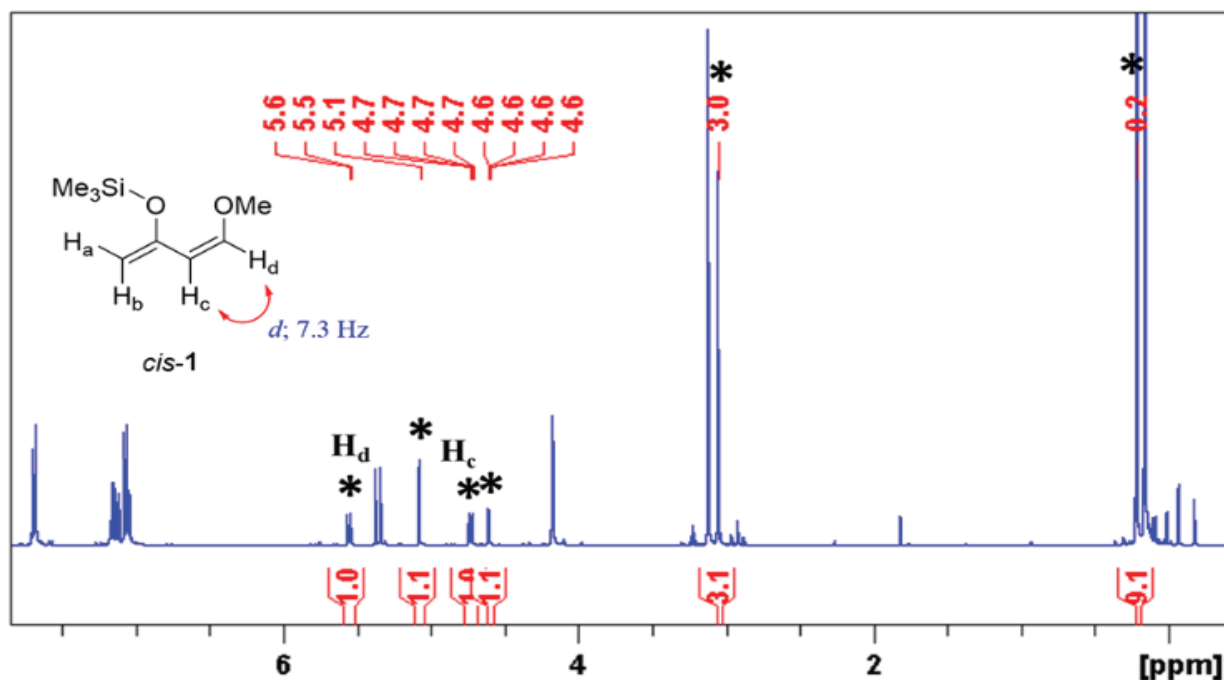
Figure 2 ^{1}H NMR (400 MHz, C_6D_6) spectra of the photochemical reaction of *trans*-**1** with **2b** after 1 hour irradiation using 365 nm LED lamp at 20°C (***** = signal of *cis*-**1**)

The signals can be assigned to the trimethylsilyl group, methoxy group, geminal alkene proton (two protons from C_1), and vicinal alkene proton (protons from C_3 and C_4), respectively. The *cis* configuration was determined based on the coupling constant of 7.3 Hz, which arose from the protons on C_3 and C_4. This is much smaller than that (12.7 Hz) of the *trans* configuration. Triplet–triplet energy transfer from **2b** to *trans*-**1** is proposed for the isomerisation, with *trans*-**1**/*cis*-**1** isomer ratio of ~ 65/35. As there are no reports on the synthesis of *cis*-**1**, this method can be considered as a new, simple, and convenient procedure to synthesise *cis*-**1**.

When the irradiation was prolonged to 12 h (Figure 1e), additional signals appeared in the regions δ 0–0.5, 2.8–3.2, 4.0–6.0, and 6.8–8.0 ppm, with a concomitant decrease in the benzophenone signal at δ ~7.8 ppm. After 24 h of irradiation (Figure 1f), no benzophenone signal was detected, indicating that the reaction reached completion with 100% conversion of benzophenone. The solvent was removed under reduced pressure, and the four major products were isolated using silica gel column chromatography. Analyses of the 1D NMR (^{1}H and ^{13}C) and 2D NMR (H-H COSY, H-C HSQC, and H-C HMBC) spectra and the mass spectra confirmed that among the 8 possible oxetanes **5-8** (Scheme 5), the four major products were oxetanes *trans*-**5**, *cis*-**5**, *trans*-**7**, and *cis*-**7**.

Scheme 5 Possible oxetanes formed in the photochemical reaction of **1** with **2b**

trans-**5**   *cis*-**5**   *trans*-**7**   *cis*-**7**

trans-**6**   *cis*-**6**   *trans*-**8**   *cis*-**8**
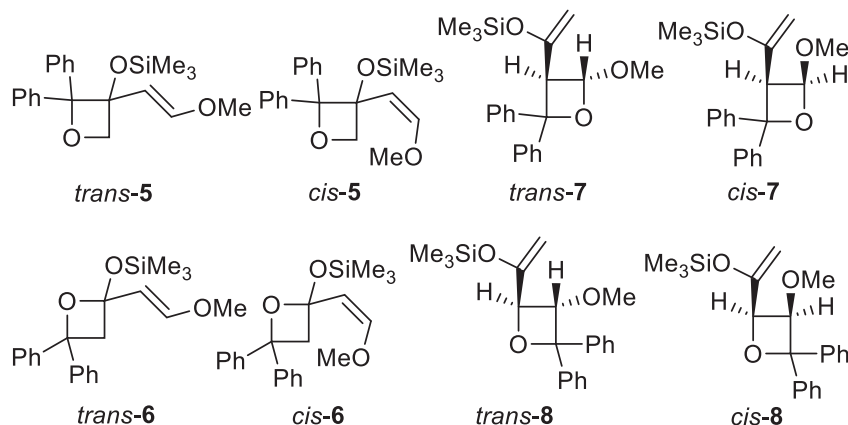
The ^{1}H NMR spectrum of *trans*-**5** is shown in Figure 1. H-C HSQC analysis clarified that the signals at δ 4.9 and 6.8 ppm appeared due to the vinylic protons. The large coupling constant of 12.7 Hz at δ 4.9 and 6.8 ppm indicates that the alkene part has a *trans*-configuration. The observation of the *trans*-configured vinylic proton excludes the possibility of formation of all the *cis* isomers and **7/8**. Furthermore, a correlation of H_e with the quaternary carbon connected to phenyl ring C_g (97.4 ppm) was observed in the H-C HMBC spectrum (Figure 4); thus, *trans*-**5** was found to be one of the four [2 + 2] cycloaddition products.
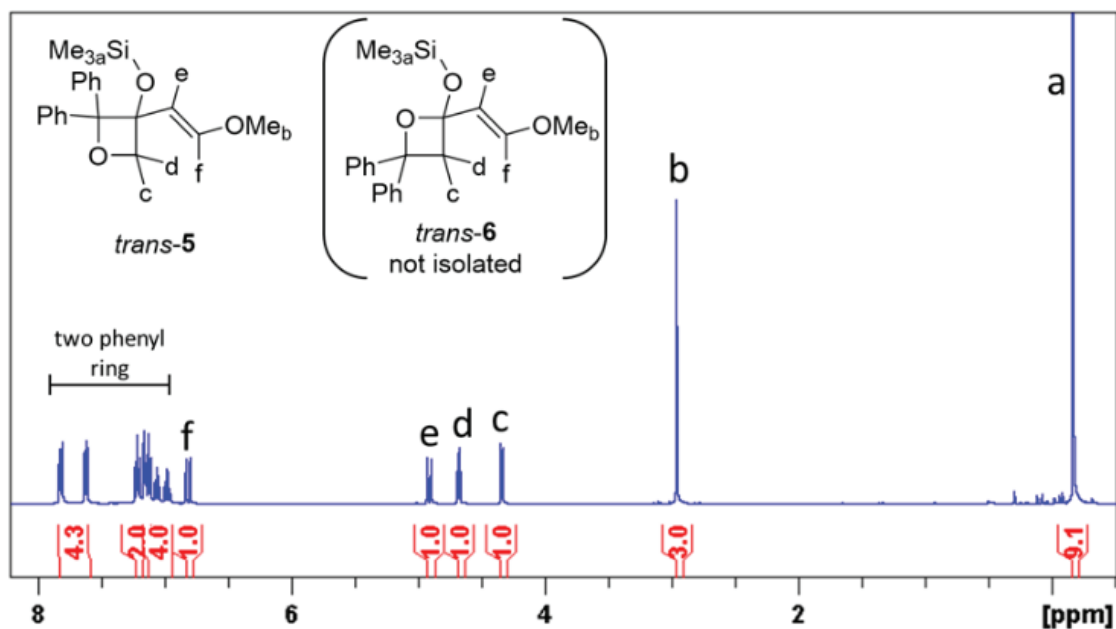
Figure 3 ^{1}H NMR (400 MHz, C₆D₆) spectra of *trans*-**5**
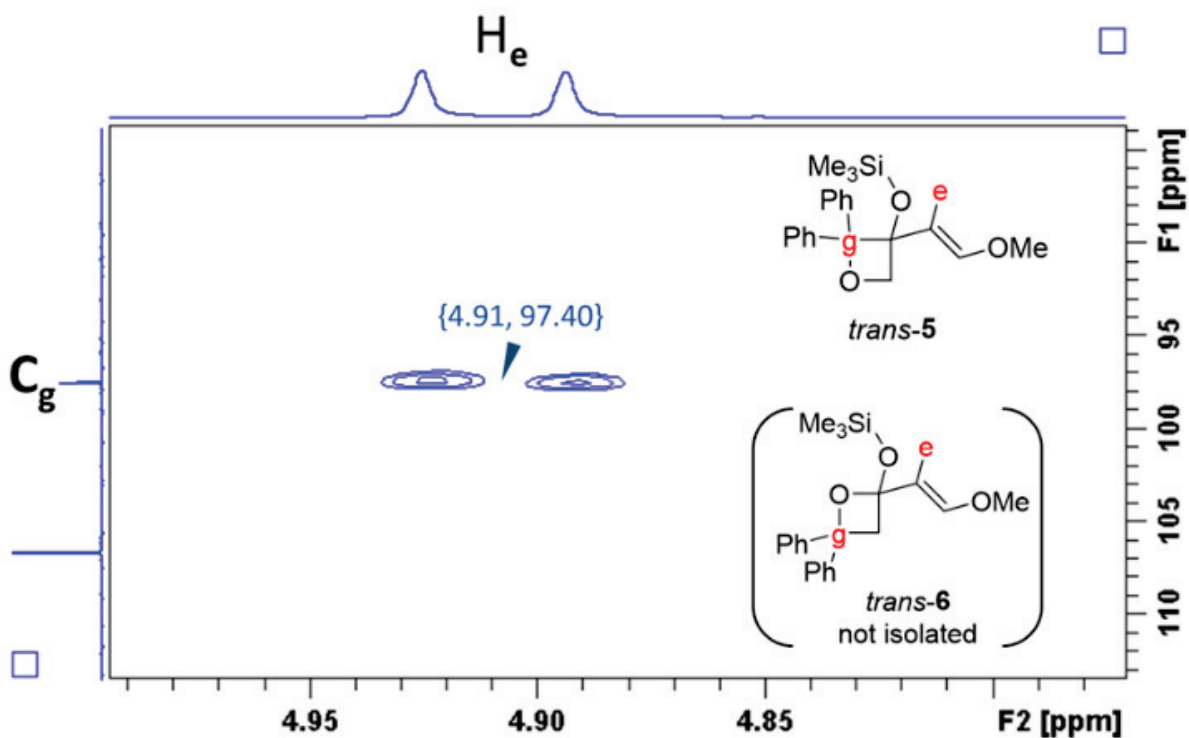
Figure 4 H-C HMBC spectra of *trans*-**5** (400 MHz, C_6D_6)

Figure 5 shows the ^{1}H NMR spectrum of *cis*-**5**. In contrast to the large coupling constant in *trans*-**5**, the protons assigned as H_e (δ 4.4 ppm) and H_f (δ 5.2 ppm) possess at coupling constant of 7.0 Hz, which is a typical value for *cis*-configuration alkene protons. The observation excludes the possibility of the formation of all-*trans* isomer and *cis*-**6/7**. The H-C HMBC spectrum (Figure 6) shows the correlation of H_e with the quaternary carbon connected to phenyl rings C_g (97.30 ppm), which verifies the formation of oxetane *cis*-**5**.
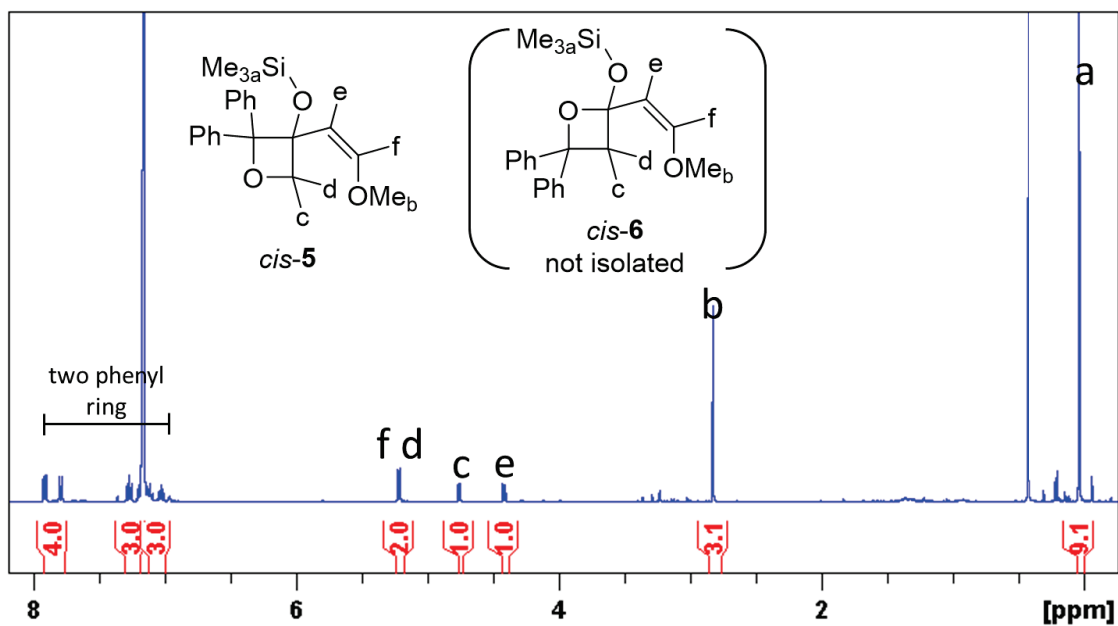
Figure 5. ^{1}H NMR (400 MHz, C$_6$D$_6$) spectrum of *cis*-**5**
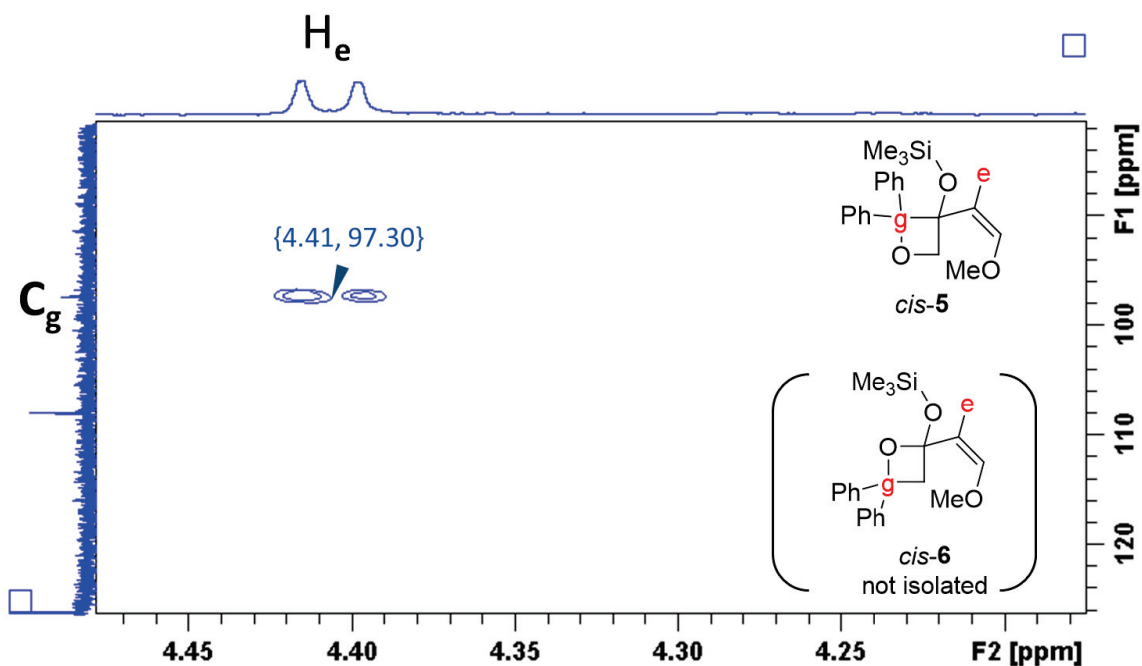
Figure 6. H-C HMBC spectrum of *cis*-**5** (400 MHz, C$_6$D$_6$)

Figure 7 shows the ^{1}H NMR spectrum of *trans*-**7**. Protons assigned as H$_c$ (δ 3.9 ppm) and H$_d$ (δ 4.1 ppm) with a very small coupling constant of 1.9 Hz belong to the alkene geminal protons. This assignment excludes the possibility of the formation of **5/6**. Moreover, in the H-

C HMBC spectrum (Figure 8), the correlation of H_e with the quaternary carbon in phenyl rings C_h (143.13 ppm) and C_i (147.70 ppm) was observed, thus excludes the possibility of the formation of *cis/trans*-**8**. The stereochemistry of proton e and f of compound *trans*-**7** was determined to be *trans* because the correlation of H_d (δ 4.11) and H_f (δ 5.79) was observed in the H-H NOESY spectrum, although the correlation of H_e and H_f was also observed. (Figure 9).
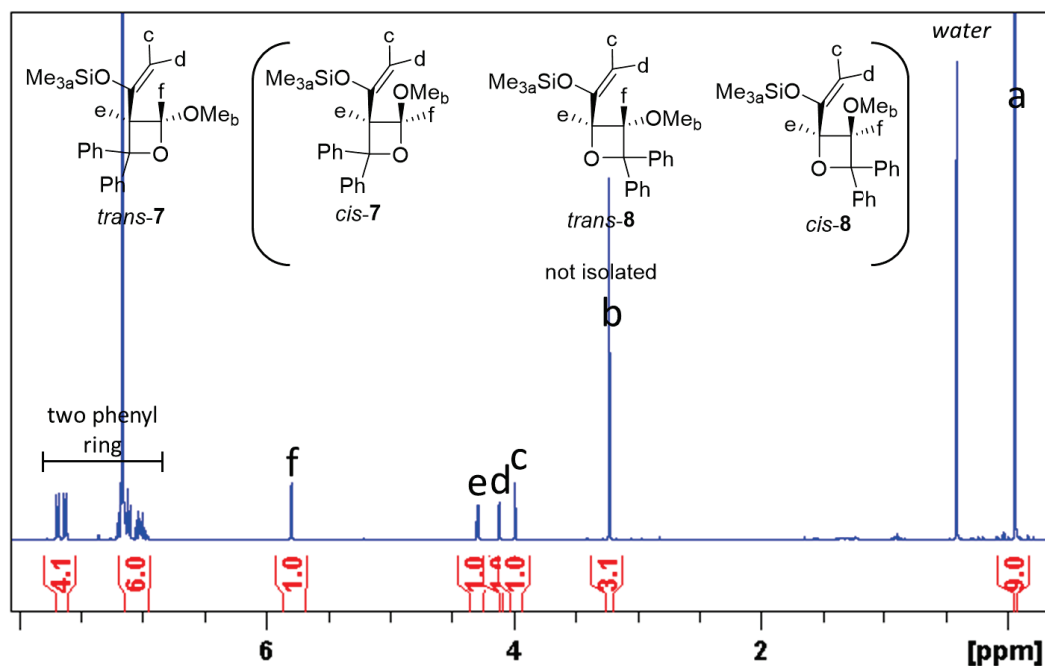
Figure 7. ^{1}H NMR (400 MHz, C_6D_6) spectrum of *trans*-**7**
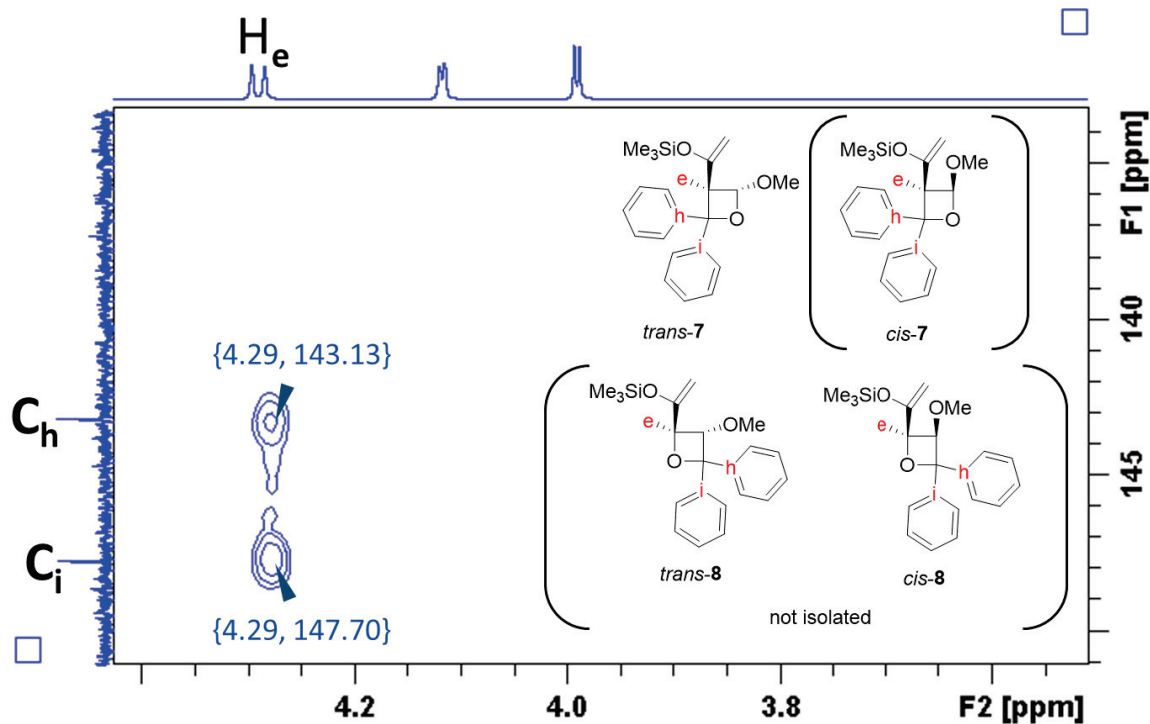
Figure 8. H-C HMBC spectrum of *trans*-**7** (400 MHz, C_6D_6)
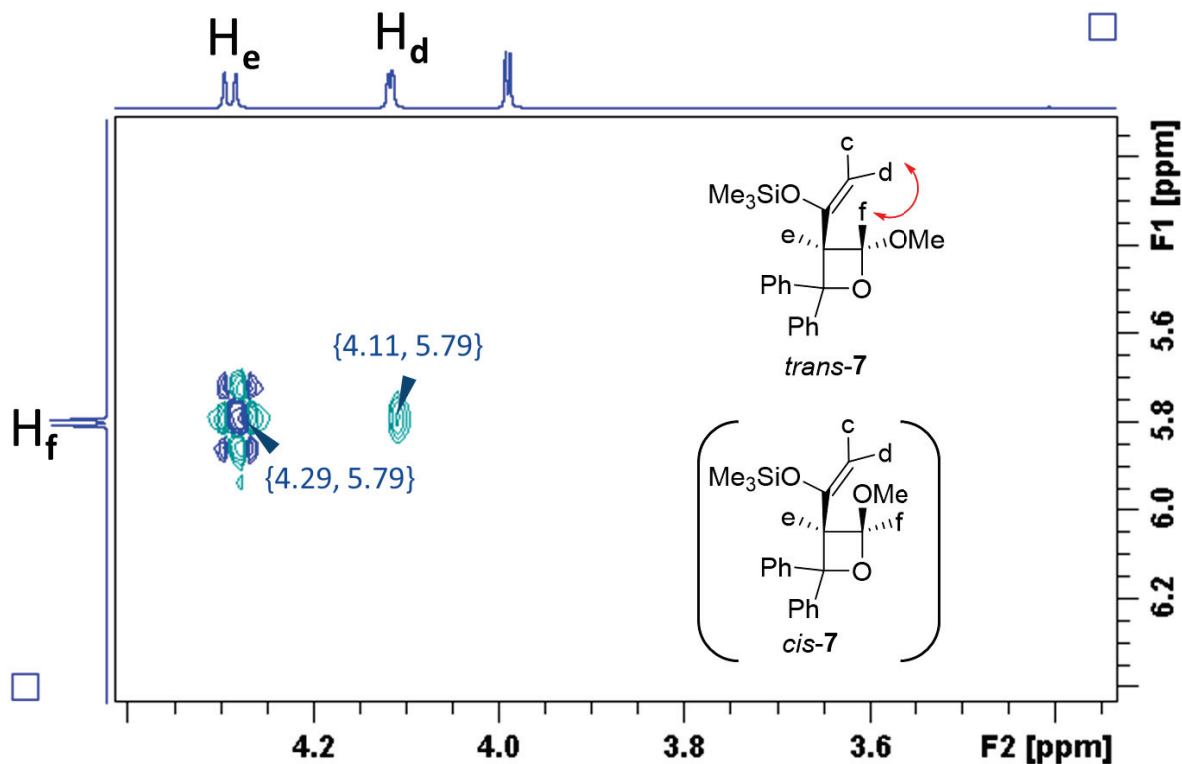
Figure 9. H-H NOESY spectrum of *trans*-**7** (400 MHz, C_6D_6)

Figure 10 shows the ^{1}H NMR spectrum of *cis*-**7**. Along with the assignment of *trans*-**7**, proton assigned as H_c (δ 4.2 ppm) and H_d (δ 4.9 ppm) with coupling constant value 1.1 Hz belong to alkene geminal proton. The observation excludes the possibility of the formation of **5/6**. Furthermore, in the H-C HMBC spectrum (Figure 11), the correlation of H_e with the quaternary carbons in phenyl rings C_h (143.22 ppm) and C_i (147.72 ppm) was observed, thus excludes the possibility of the formation of *cis/trans*-**8**. The stereochemistry of proton e and f of compound *cis*-**7** was determined to be *cis* because the correlation of H_e (δ 4.28) and H_f (δ 5.21) was observed in the H-H NOESY spectrum, but no correlation of H_d (δ 4.89) and H_f (δ 5.21) was observed. (Figure 12).
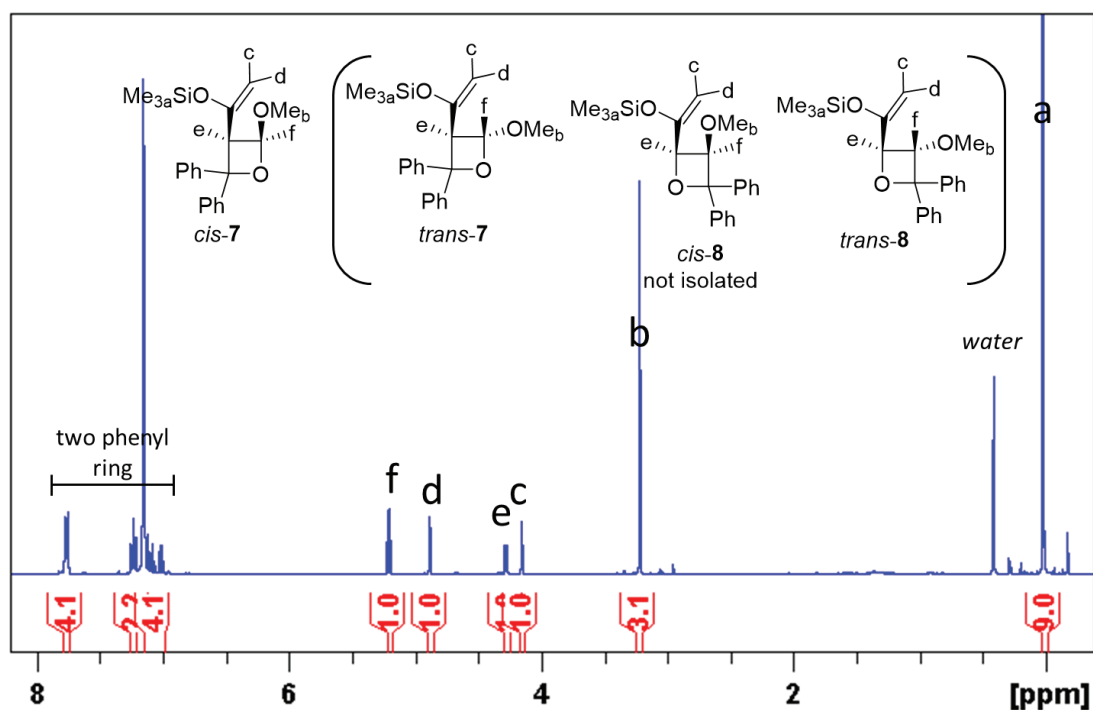
Figure 10. ^{1}H NMR (400 MHz, C$_6$D$_6$) spectrum of *cis*-**7**
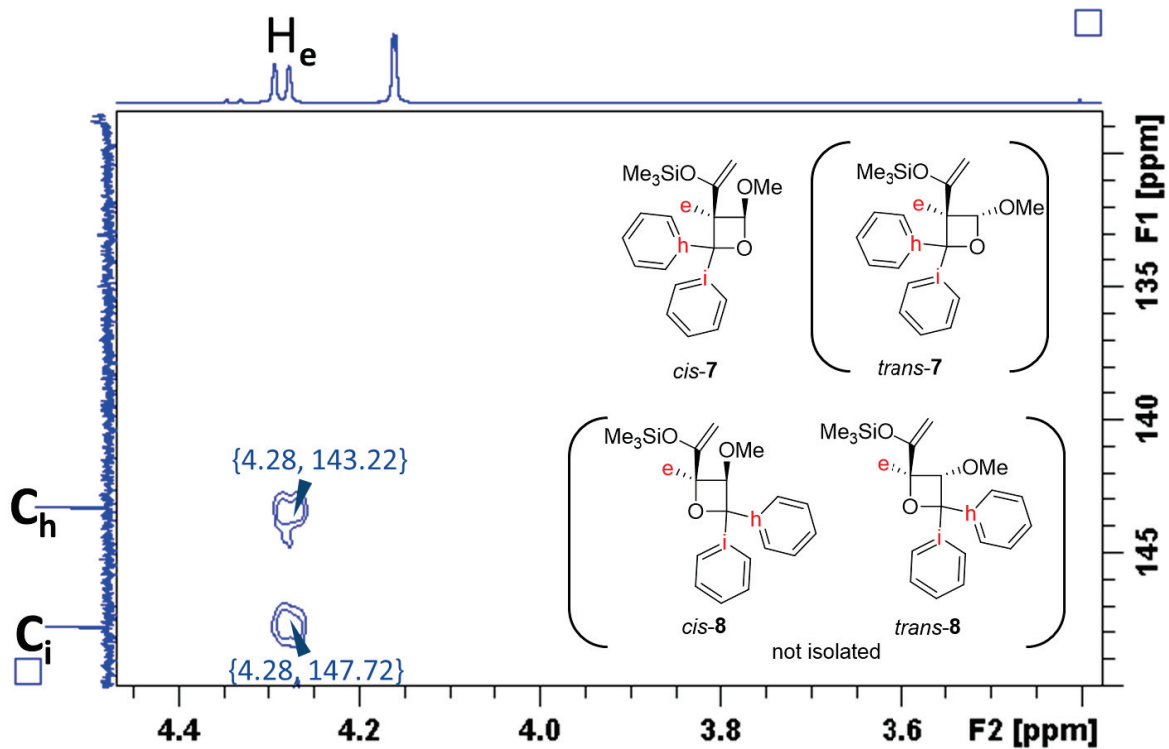
Figure 11. H-C HMBC spectrum of *cis*-**7** (400 MHz, C$_6$D$_6$)
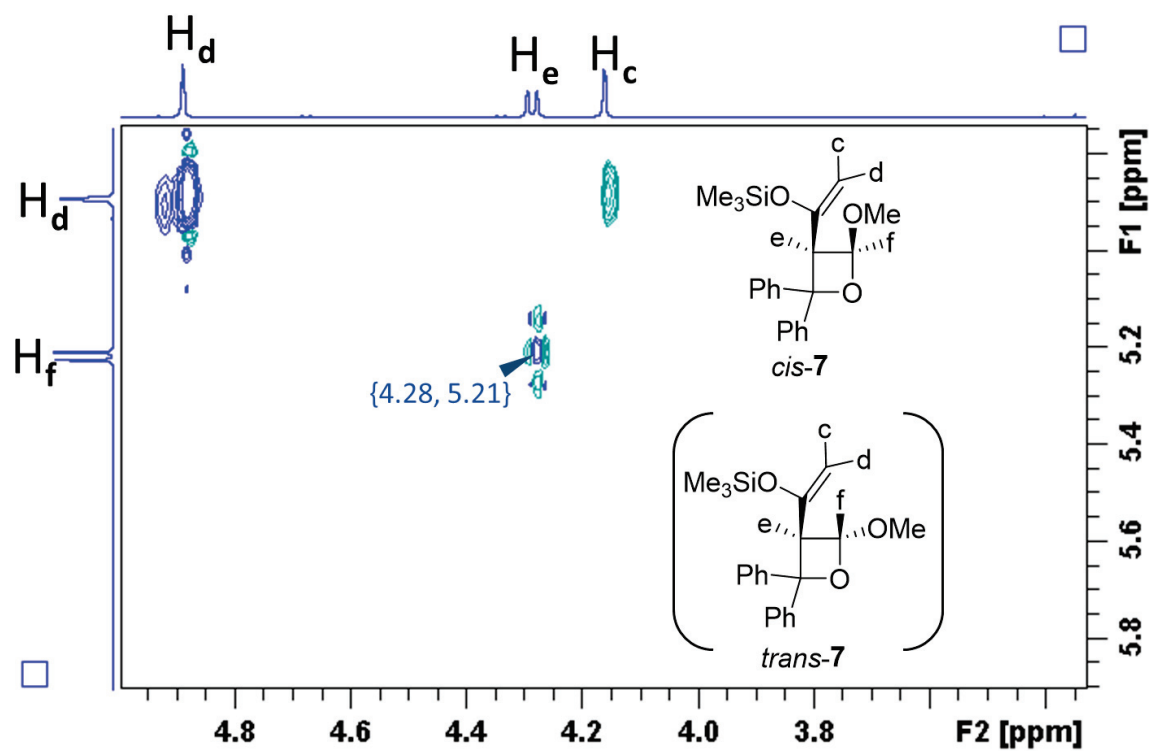
Figure 12. H-H NOESY spectrum of *cis*-**7** (400 MHz, C$_6$D$_6$)

The effects of solvent and temperature were examined on the product distribution (Table 1). The product ratio **5/7** was ~40/60 and was not largely affected by the solvent polarity (entries 1-4), suggesting that the 1,4-diradicals are more likely the intermediates than the radical ion pairs. The *cis*-selectivity of **7** increased slightly with decreasing reaction temperature. For instance, the product ratio was 46/54 at 60 °C (entry 7) and 35/65 at −78 °C (entry 5). The photolysis of benzaldehyde (**2a**) with trans-**1** produced relatively complex products.

Table 1 The photoreactions of **1** with **2b** in various solvents and temperature

Entry	Solvent	Temperature	% yield of product[a]				Product ratios[b]
		(°C)	*trans*-**5**	*cis*-**5**	*trans*-**7**	*cis*-**7**	(**5/7**)
1	Benzene	20	32	5	32	14	44/56
2	Acetonitrile	20	36	6	40	9	46/54
3	Acetone	20	39	5	45	10	44/56
4	Toluene	20	27	5	31	12	43/57
5	Toluene	−78	27	4	30	27	35/65
6	Toluene	0	29	4	31	15	42/58
7	Toluene	60	26	4	27	8	46/54

Reaction conversion was 100% (no recovered **2b**) after 24-h irradiation. [a] % yield of product was determined based on ^{1}H NMR peak using triphenylmethane as the internal standard (error $\pm$ 3%). [b] The ratios were normalized to 100%

To gain information on the mechanism of the photochemical reaction, time resolve absorption spectroscopy analyses were carried out using a laser flash photolysis (LFP) method with 355 nm Nd: YAG laser (4 ns pulse-width, 6 mJ/pulse). The triplet benzophenone ^{3}**2b*** was observed at λ_{max} ~535 nm just after the lase flash. The fall process (k_d, [**1**] = 0 mM) to the ground state was monitored at 535 nm at 298 K under N_2 (Figure 13). The rate constant for the quenching (k_q) of triplet-state **2b** (^{3}**2b***) by **1** was determined by monitoring the 535 nm signals (k_{obs}). The quenching rate constant k_q was obtained from the Stern–Volmer plot (k_{obs}/k_d =1+(k_q/k_d)), which was obtained from the LFP data acquired at 355 nm in a degassed benzene solution [**1**]. Under the conditions of LFP, only **2b** was electronically excited, because compound **1** does not absorb at wavelengths longer than 300 nm (Figures 14, 15). The lifetime of the transient ^{3}**2b*** species was significantly reduced in the presence of **1** (Figure 13, Table 2). The Stern–Volmer plot (Figure 16) was obtained by plotting k_{obs} as a function of [**1**]. The rate constant for quenching (k_q) of **1** by **2b** was determined to be 7.8 x 10^8 M^{-1}s^{-1} from the

Stern–Volmer plot. The quenching rate constant of ^{3}**2b*** in the presence of 0.6 M **1** is 0.47 x 10^9 s^{-1}. The decay rate constant (k_d) of ^{3}**2b*** alone is ~1.6 x 10^5 s^{-1}.[8] Although the quenching rate constant (k_q) was relatively high, the quantum yield (Φ) for the formation of oxetane product was quite low (Φ = 1.7 x 10^{-3}). The number of photons were determined using the ferrioxalate actinometer (Figure 25-26 and Table 3). Thus, energy transfer from ^{3}**2b*** to *trans*-**1** is the main quenching pathway of ^{3}**2b*** to generate ^{3}*trans*-**1***, which further isomerises to *cis*-**1**.
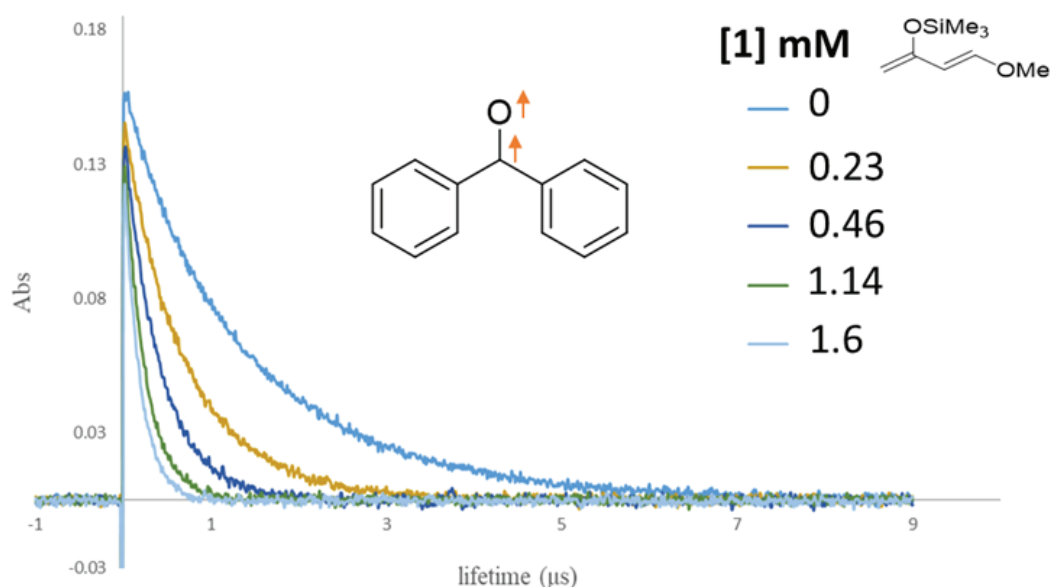
Figure 13 Decay curves of ^{3}**2b*** at 535 nm, which was generated by 355-nm laser flash photolysis in degassed benzene solution in the presence of **[1]** at 298 K

Table 2 The decay rate constant of ^{3}**2b*** in the presence of *trans*-**1**

[*trans*-**1**] (mM)	k_{obs}
0.00	6.1 x 10^5
0.23	13.4 x 10^5
0.46	22.5 x 10^5
1.14	43.0 x 10^5
1.60	54.1 x 10^5
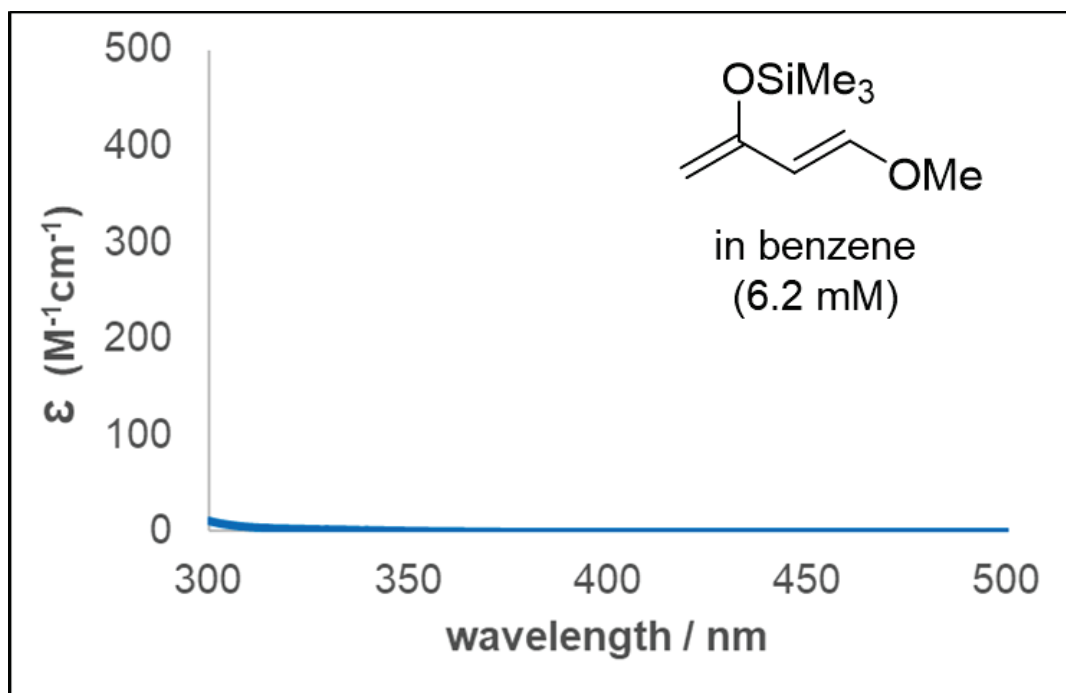
Figure 14. UV spectrum of *trans*-**1**
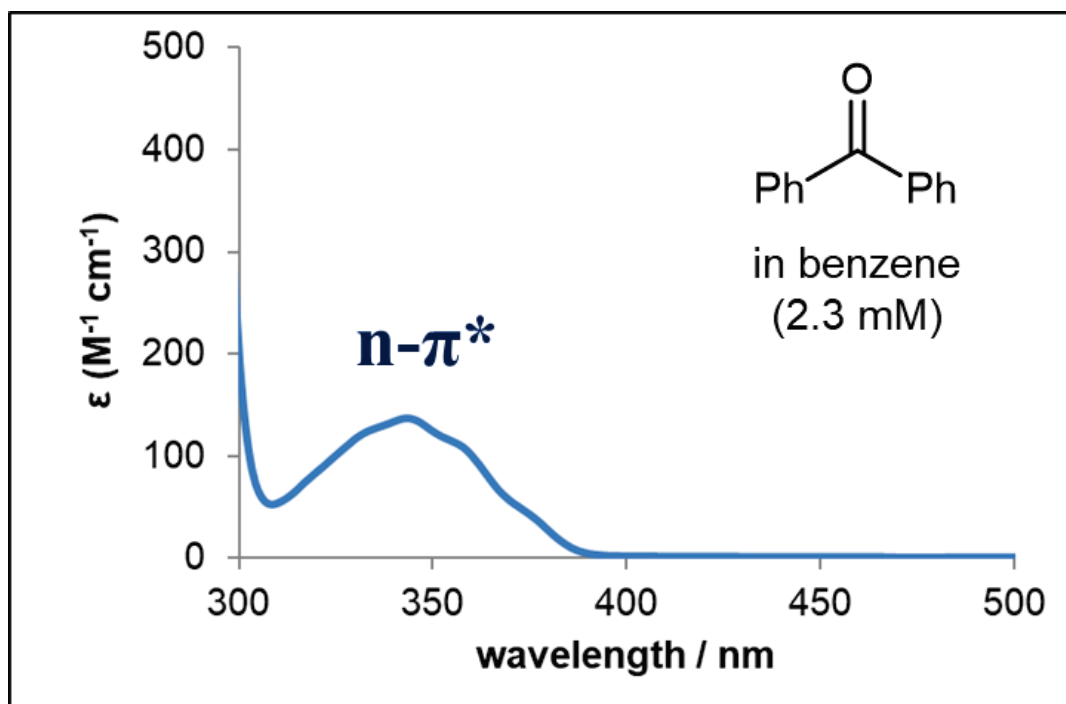
Figure 15. UV spectrum of **2b**

Stern Volmer plot of **1**
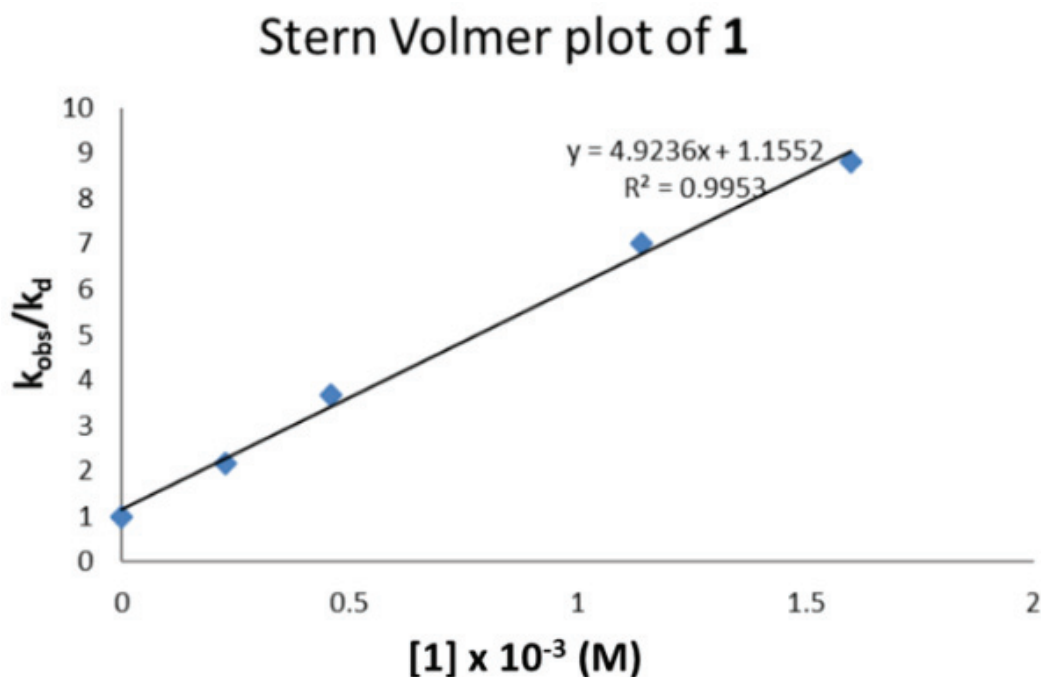
Figure 16 The Stern–Volmer plot ($k_{obs}/k_d = 1 + k_q/k_d \, [\mathbf{1}]$) for the quenching reaction of $^3\mathbf{2b}^*$ by **1** in degassed benzene at room temperature

A plausible mechanism for the formation of oxetane in the photoreaction of *trans*-**1** with **2b** is shown in Scheme 6. When **2b** absorbs light of 365 nm, electronic excitation from the n orbital into the π* orbital of C=O bond occurs. This is followed by a fast intersystem crossing (ISC) that produces the triplet excited state benzophenone $^3\mathbf{2b}^*$. The triplet energy transfer from $^3\mathbf{2b}^*$ to *trans*-**1** initiates the isomerisation of the C_3-C_4 double bond to produce *cis*-**1**. The energy of the excited state benzophenone is 69 kcal mol^{-1}.[8] The triplet state energy of **1** was computed to be ~51 kcal mol^{-1}, indicating that the energy transfer from $^3\mathbf{2b}^*$ to **1** for forming $^3\mathbf{1}^*$ is possible. In the first 1 h of irradiation, the *trans-cis* isomerisation resulted in a *trans/cis* ratio of 65/35, indicating that this process is more efficient than the other chemical reactions.

Scheme 6 General scheme of the Paternò–Büchi reaction of **1** with **2b**
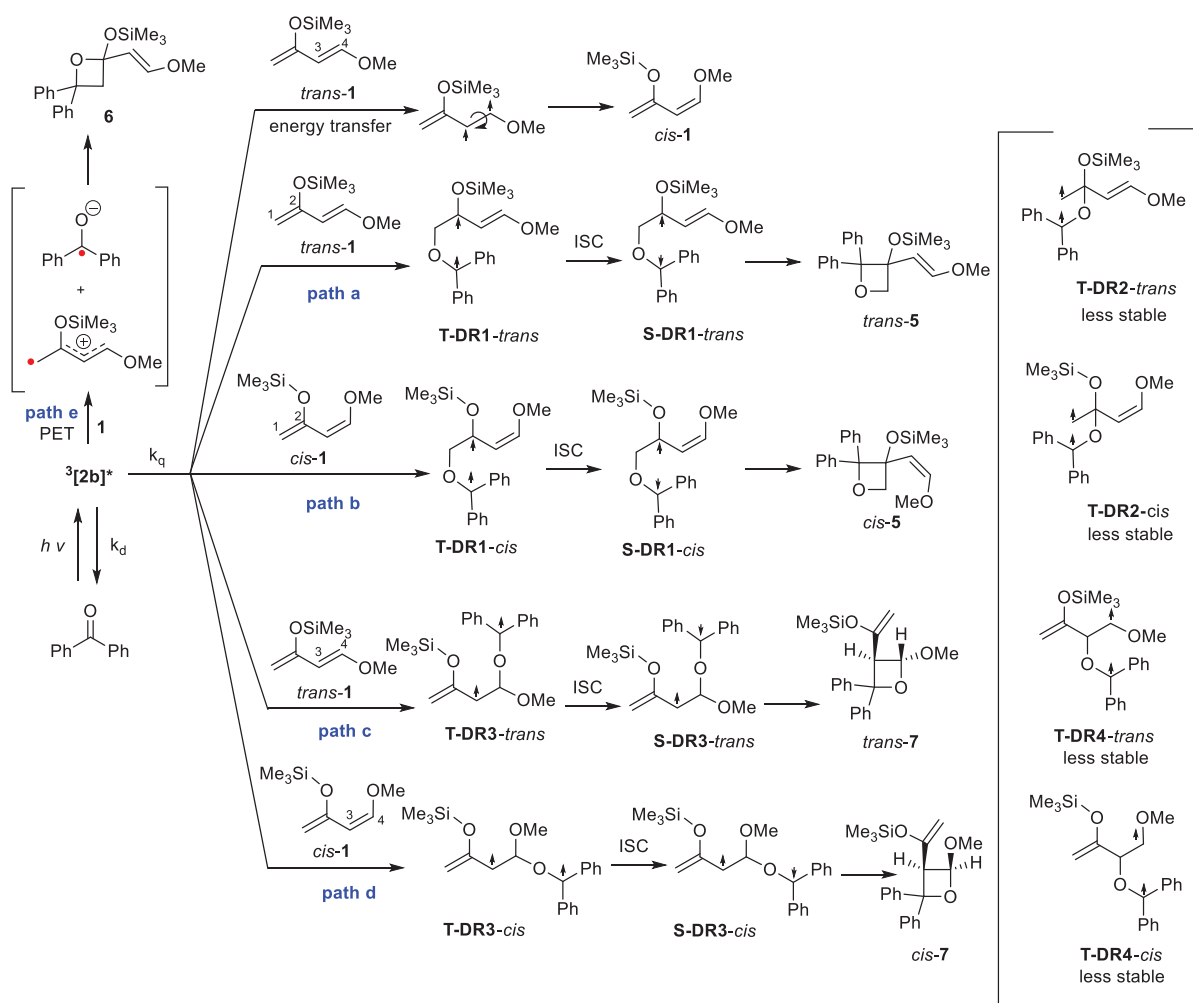
The long-lived triplet excited state of **2b** can react intermolecularly with **1** to give the intermediary triplet diradicals (Scheme 6). The C1 carbon atom of *trans*-**1** reacts with the electrophilic oxygen of ^{3}**2b*** to generate the intermediary triplet 1,4-diradical **T-DR1**-*trans* (path a). The C1 carbon atom in *trans*-**1** is more nucleophilic than the other carbon atoms owing to its higher HOMO coefficient as compared to other carbon atoms. Calculations predict that intermediaries **TDR-2** and **TDR-4** are less stable than **TDR-1** and **TDR-3**, because the latter two can exist in additional resonance forms. After the ISC to **S-DR1**-*trans*, oxetane *trans*-**5** is produced. The *cis* diene, *cis*-**1**, can also react with ^{3}**2b*** to produce the intermediary triplet 1,4-diradical **T-DR1**-*cis* (path b). After the ISC to **S-DR1**-*cis*, oxetane *cis*-**5a** is produced. The $C_3=C_4$ double bond in *trans*-**1** can also react with ^{3}**2b*** to produce the intermediary triplet 1,4-diradical **T-DR3**-*trans* (path

29

c). After the ISC to **S-DR3**-*trans*, oxetane *trans*-**7** is formed. The C_4 carbon atom of *cis*-**1** reacts with **^{3}2b*** to produce the intermediary triplet 1,4-diradical **T-DR3**-*cis* (path d). After the ISC to **S-DR3**-*cis*, oxetane *cis*-**7** is formed.

As mentioned above, the formation of the 1,4-diradical intermediates, which can be generated in the reaction of the electrophilic oxygen of carbonyl with the nucleophilic diene, is reasonable to understand the observed regioselectivity. When the PET reaction occurs from **1** to ^{3}[**2b**]*, the radical ion pair is formed (path e). The electron transfer process is possible, as judged by the low oxidation potential of **1** (+0.9 V versus Ag/Ag$^+$) and the high reduction potential of ^{3}[**2b**]* (–1.8 V versus Ag/Ag$^+$ (Figure 17). However, a large spin density of 0.67 was found to be localized at C1 carbon in the radical cation of **1**, which was computed at the UB3LYP/6-31G(d) level of theory (Figure 18). The value of 0.13 was calculated at C3 carbon. The cation charge was delocalized in C2 and C4 carbons. Thus, the radical ion pair should produce oxetane **6** (path e), which is not consistent with the experimental observation. At this moment, we hypothesize that the electron transfer process is in the Marcus inverted region.[9]
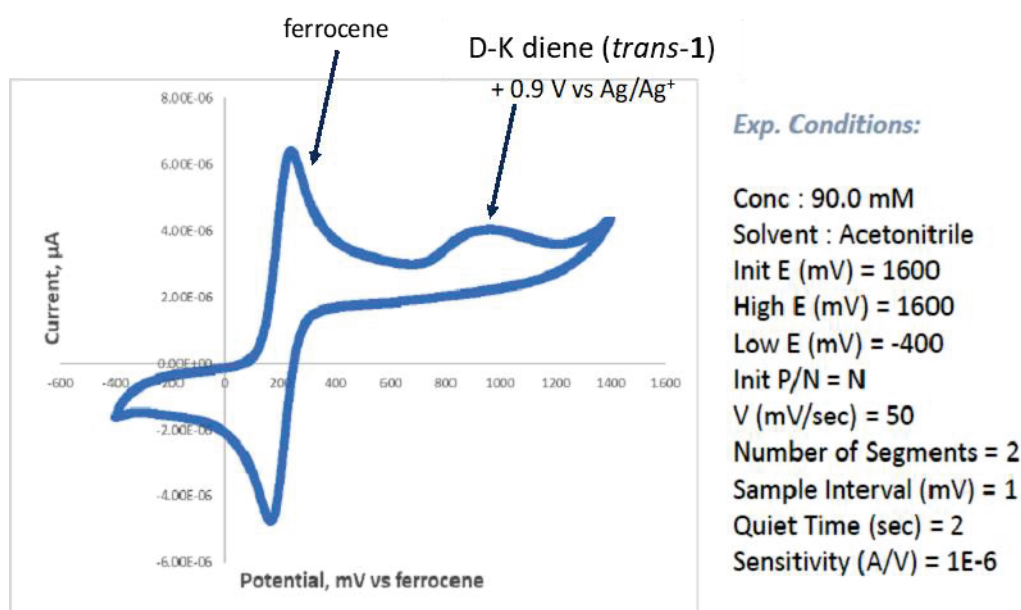
Figure 17. Cyclic voltammetry measurement of Danishefski-Kitahara diene (1).

		Charge	spin density
1	C	0.113530	0.669493
4	C	0.491633	-0.073725
5	O	-0.595433	0.030489
6	Si	0.867500	-0.003619
7	C	-0.098302	0.000051
11	C	-0.116720	0.001795
15	C	-0.116877	0.001792
19	C	-0.025338	0.133408
21	C	0.436866	0.119367
23	O	-0.359149	0.115964
24	C	0.402292	0.004985
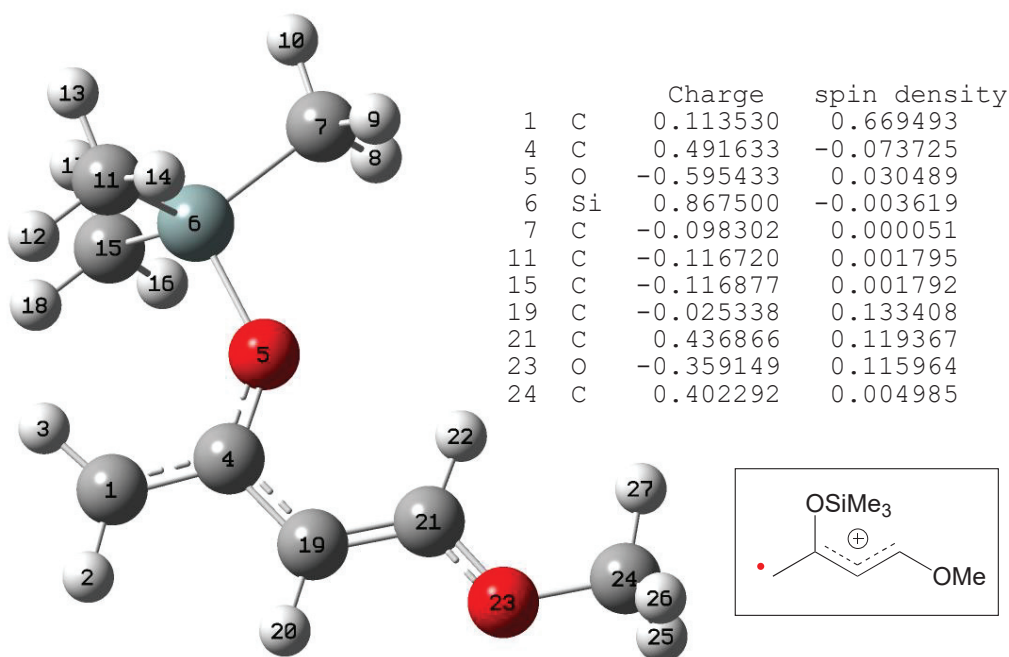
Figure 18. Charge and spin-density distribution in the radical cation of 1 at the UB3LYP/6-31G(d) level of theory.

Table 1 shows that the *trans* isomers are the major products in the formation of oxetanes **5** and **7**. The *trans*-selectivity can be explained by the higher ratio of *trans*-isomer in the starting compound **1**. To gain insights into the selection of double bonds, i.e., $C_1=C_2$ versus $C_3=C_4$, computational calculations were performed on the triplet intermediaries **T-DR1**-*trans* and **T-DR3**-*trans* (Scheme 7). The computations on the *cis* isomer are shown in Scheme 8 and Figure 20. Two energy minima corresponding to gauche and anti conformers were found in each of the triplet diradicals. The gauche conformers can produce oxetane products **5** and **7** after ISC, while the anti conformer goes back to the starting materials **1** and **2b**. The population of the productive gauche conformers among all the conformers is considered to affect the product selectivity (Eqn 1).[10] The potential energy surfaces (PESs) around the dihedral angle θ (deg) were calculated for **T-DR1**-*trans* and **T-DR3**-*trans* at the UB3LYP/6-31G level of theory (Figure 19). The triplet diradical **T-DR1** was found to be energetically more stable than **T-DR3** by 10–25 kJ mol^{-1}. The energy-minimum gauche conformers (θ = ~60° for **T-DR3**-*trans* and θ = ~300° for **T-DR1**-*trans*) were found on the PESs. As mentioned before, the anti conformers **T-DR1**-anti-*trans* and **T-DR3**-anti-*trans* go back to form the starting compounds after ISC. On the other hand, the gauche conformers **T-DR1**-gauche-*trans* and **T-DR3**-gauche-*trans* can be transformed into the oxetane products. However, the productive gauche conformer was calculated to be less stable than the unproductive anti conformer by 5.0–20.0 kJ mol^{-1}.

31

Calculations predict that oxetane **5**, which is derived from **T-DR1**, would be the major product. However, almost a 50:50 ratio was observed experimentally.

Scheme 7. Proposed mechanism for the selective formation of *trans*-**5** and *trans*-**7**
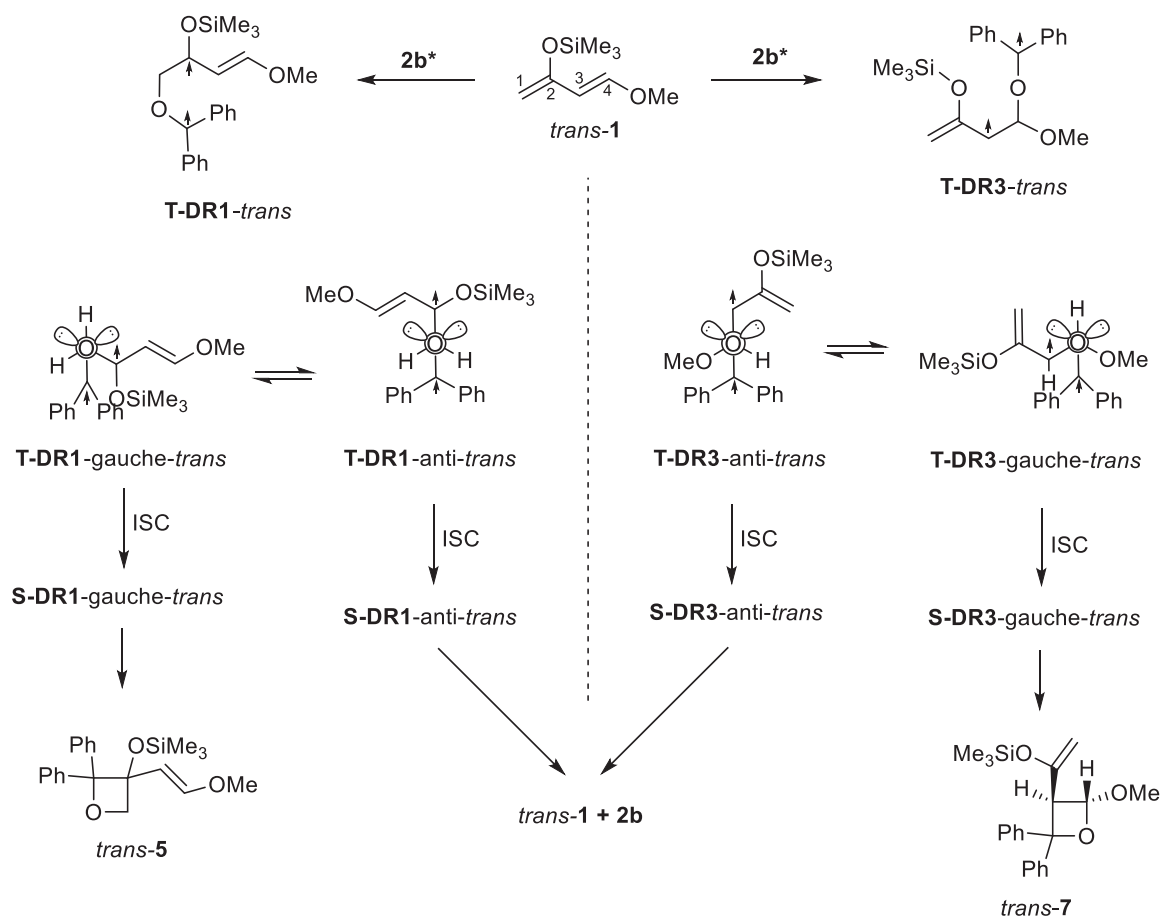
$$5 : 7 = \frac{[\textbf{T-DR1}\text{-gauche-}\textit{trans}]}{[\textbf{T-DR1}\text{-gauche-}\textit{trans}] + [\textbf{T-DR1}\text{-anti-}\textit{trans}]} : \frac{[\textbf{T-DR3}\text{-gauche-}\textit{trans}]}{[\textbf{T-DR3}\text{-gauche-}\textit{trans}] + [\textbf{T-DR3}\text{-anti-}\textit{trans}]} \quad (1)$$

Scheme 8. Proposed mechanism for the selective formation of *cis*-**5** and *cis*-**7**
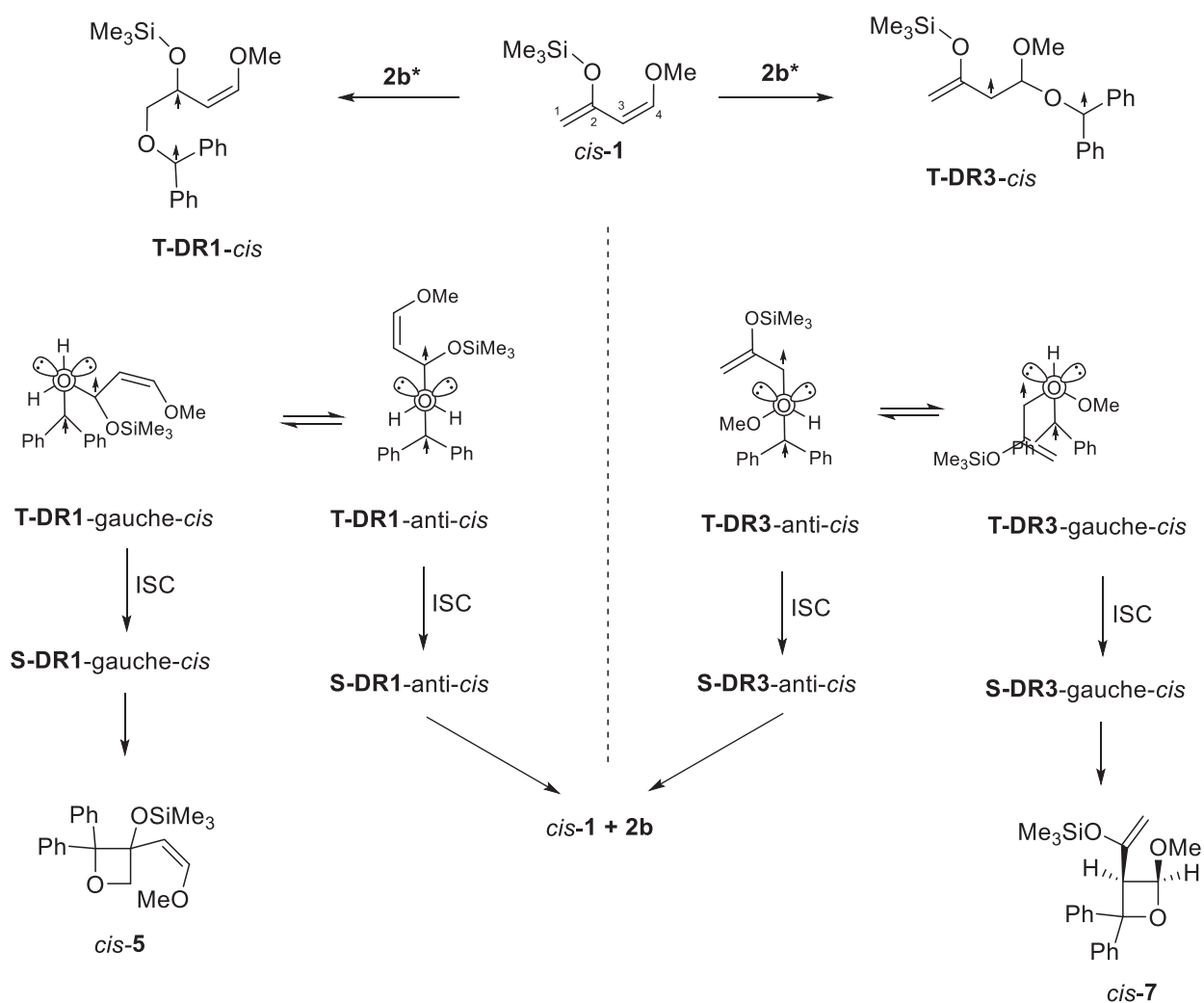
$$5 : 7 = \frac{[\text{T-DR1}\text{-gauche-}cis]}{[\text{T-DR1}\text{-gauche-}cis] + [\text{T-DR1}\text{-anti-}cis]} : \frac{[\text{T-DR3}\text{-gauche-}cis]}{[\text{T-DR3}\text{-gauche-}cis] + [\text{T-DR3}\text{-anti-}cis]} \quad (1)$$
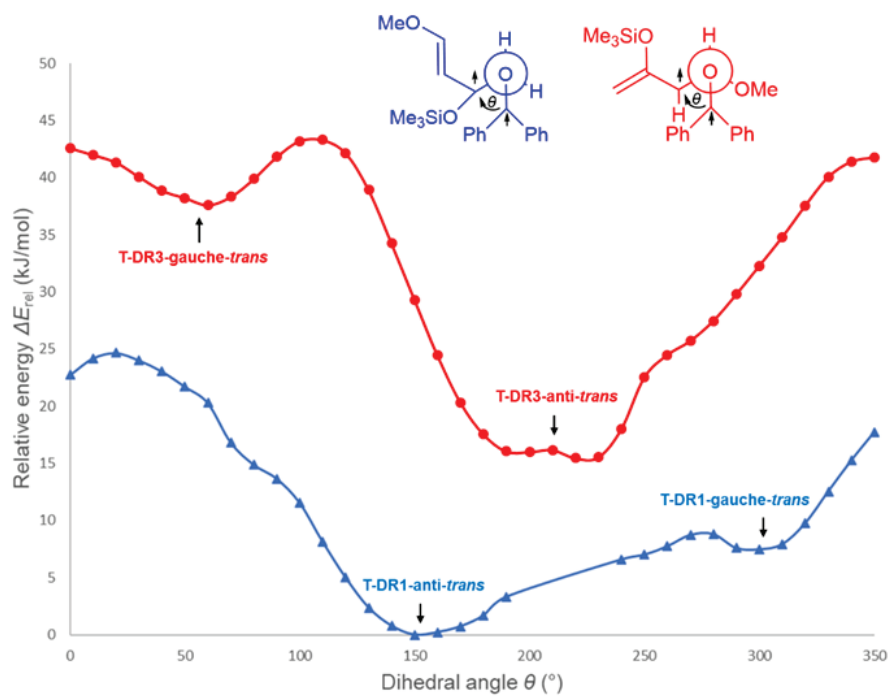
Figure 19 PES analyses around the dihedral angle ($\theta°$) of diradicals **T-DR1**-*trans* and **T-DR3**-*trans*. The energies, ΔE_{rel} in kJ/mol, were relative to the most stable conformer.
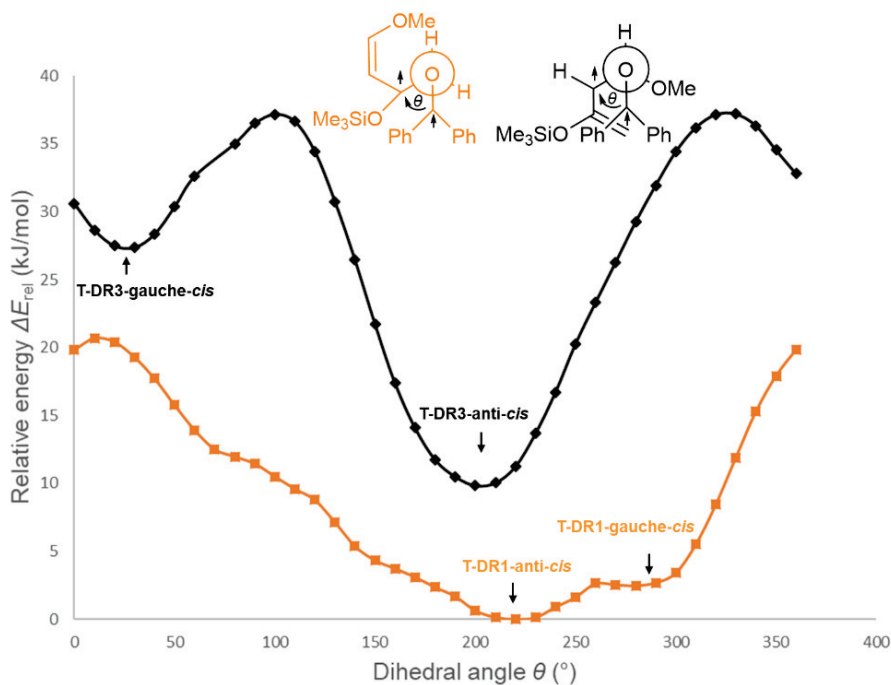
Figure 20 PES analyses around the dihedral angle ($\theta°$) of diradicals **T-DR1**-*cis* and **T-DR3**-*cis*. The energies, ΔE_{rel} in kJ/mol, were relative to the most stable conformer.

To gain further insights into the double-bond selection, the energy barriers for bond formation in the reaction of ^{3}**2b*** with *trans*-**1** and *cis*-**1** were examined. The simulation was performed by considering the reaction of triplet state acetone with *trans*-**1b** (Figure 21) and *cis*-**1** (Figure 22) as a model reaction. Figure 23 and Figure 24 clearly shows that the formation of diradicals **T-DR1** and **T-DR3** was a barrier-less process, indicating that there was no double bond selection in the addition reaction. When the molecular structures were carefully checked, the electrophilic oxygen and the singly-occupied *n*-orbital were found to interact preferably with the occupied orbitals of the $C_1=C_2$ and $C_3=C_4$ double bonds (Figure 23). The perpendicular structures during the C_1-O bond formation produced the gauche conformation of the resulting triplet diradicals. The perpendicular orientation accelerates the ISC to give the corresponding singlet state that produces the oxetane compounds.[11] The computational studies indicate that the first step of the reaction, that is, the addition of the triplet state acetone to *trans*-**1b**, is not regioselective. Thus, the triplet diradicals **T-DR1** and **T-DR3** should be formed in equal proportion in the reaction of the triplet state acetone with *trans*-**1b**.
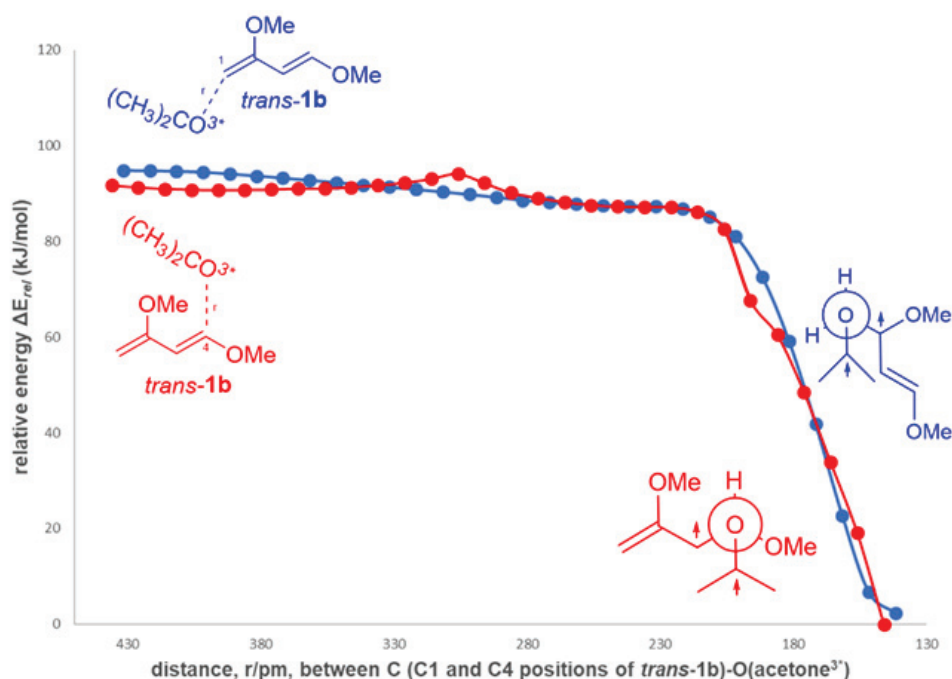
Figure 21. The UB3LYP/6-31G(d) potential energy surface analyses of the distance r (pm) of the C (C1 and C4 position of *trans*-**1b**) to the O of **acetone**. The energies, ΔE_{rel} in kJ/mol, are relative to the most stable diradical.
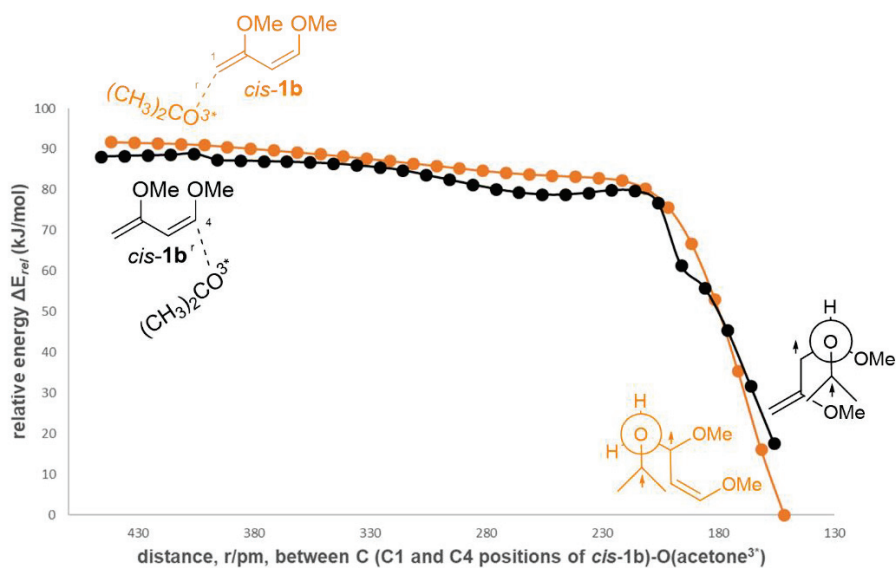
Figure 22. The UB3LYP/6-31G(d) potential energy surface analyses of the distance r (pm) of the C (C1 and C4 position of *cis-1b*) to the O of **acetone**. The energies, ΔE_{rel} in kJ/mol, are relative to the most stable diradical.
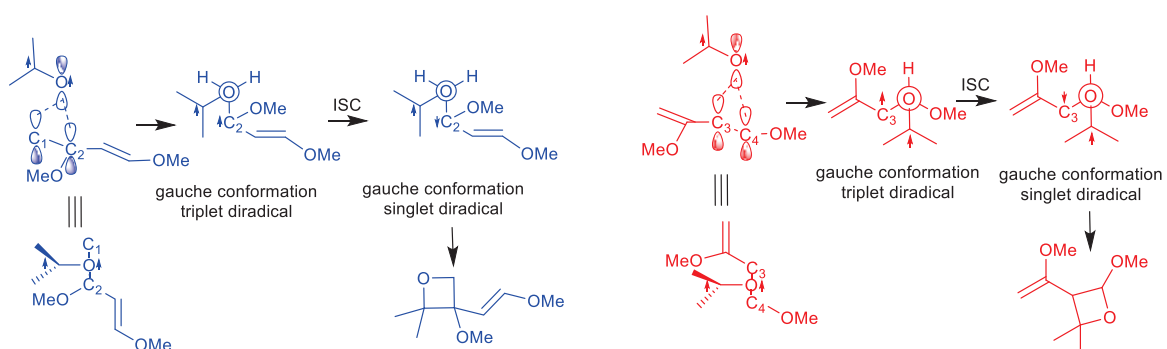
Figure 23. The bond formation of the C-O produced the gauche conformation of the resulting triplet diradicals to give the corresponding singlet state that produces the oxetane

2.3 Experimental section

General information

All the reagents and solvents were obtained at reagent grade. Thin-layer chromatography (TLC) analysis was performed on silica gel plates and viewed under ultraviolet light. ^{1}H NMR and ^{13}C NMR data were recorded with a 400 MHz NMR spectrometer. C_6D_6 was used as deuterated solvents. Chemical shifts were described in parts per million (ppm) relative to the residual C_6H_6 (7.16 ppm), and the coupling constants (J) was stated in Hertz (Hz). The product yields were determined using peak areas (error $\pm 3\%$) of triphenylmethane (Ph_3CH) as an internal standard. Comparisons of the peak areas determined the product ratios. High-resolution Mass (HRMS) spectroscopic analyses were conducted using an Orbitrap XL instrument using the positive ion mode.

General procedure for the photoreaction of *trans*-1 and 2b

A degassed benzene solution of *trans*-1 (0.3 mmol) and 2b (0.1 mmol) in Pyrex NMR tube was irradiated by light-emitting diode (LED) at 365 nm for 24 h. After removing the solvent, the products were separated by flash column chromatography on silica gel (SiO_2, EtOAc/n-hexane).

Laser flash photolysis (LFP) measurements

The excitation source for the LFP system was an Nd: YAG laser, the third-harmonic of a 1064 nm. The monitoring system consisted of a 150 W xenon lamp as light source, Unisoku-MD200 monochromator, and a photomultiplier.

Computational method

The reaction profiles and geometry optimization were calculated at the (U)B3LYP/6-31G(d) level of theory[12–14] using the Gaussian 09 suite programs[15].

(Z)-((4-methoxybuta-1,3-dien-2-yl)oxy)trimethylsilane (cis-1).
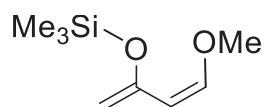
¹H NMR (400 MHz, benzene-*d₆*) δ 5.55 (d, *J* = 7.3 Hz, 1H), 5.08 (s, 1H), 4.73 (dd, *J* = 1.8 Hz, *J* = 7.3 Hz, 1H), 4.61 (dd, *J* = 0.5 Hz, *J* = 1.7 Hz, 1H), 3.05 (s, 3H), 0.21 (s, 9H). ¹³C NMR (101 MHz, benzene-*d₆*) δ 152.4, 148.3, 104.5, 95.9, 59.7, -0.1.

(E)-((3-(2-methoxyvinyl)-2,2-diphenyloxetan-3-yl)oxy)trimethylsilane (*trans*-5).
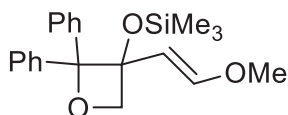
¹H NMR (400 MHz, benzene-*d₆*) δ 7.82 (d, *J* = 7.9 Hz, 2H), 7.62 (d, *J* = 7.8 Hz, 2H), 7.21 (t, *J* = 7.6 Hz, 2H), 7.13 (t, *J* = 7.6 Hz, 2H), 7.06 (t, *J* = 7.4 Hz, 1H), 6.98 (t, *J* = 7.4 Hz, 1H), 6.82 (d, *J* = 12.7 Hz, 1H), 4.91 (d, *J* = 12.6 Hz, 1H), 4.68 (d, *J* = 6.0 Hz, 1H), 4.34 (d, *J* = 6.0 Hz, 1H), 2.96 (s, 3H), -0.17 (s, 9H). ¹³C NMR (101 MHz, benzene-*d₆*) δ 148.21, 144.33, 142.74, 127.55, 126.54, 126.50, 126.28, 125.53, 106.54, 97.40, 79.69, 78.64, 54.93, 0.76. HRMS m/z: [M+H]⁺ anal. calcd for C₂₁H₂₇O₃Si 355.17295, found 355.17267.

(Z)-((3-(2-methoxyvinyl)-2,2-diphenyloxetan-3-yl)oxy)trimethylsilane (*cis*-5).
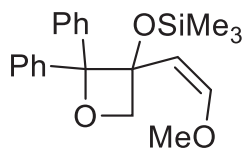
¹H NMR (400 MHz, benzene-*d₆*) δ 7.92-7.89 (m, 2H), 7.80-7.76 (m, 2H), 7.29-7.24 (m, 2H), 7.20-7.17 (m, 1H), 7.13-7.08 (m, 2H), 7.04-6.99 (m, 1H), 5.22 (d, *J* = 7.0 Hz, 1H), 5.21 (d, *J* = 6.1 Hz, 1H), 4.76 (dd, *J* = 0.7 Hz, *J* = 6.0 Hz, 1H), 4.42 (dd, *J* = 0.7 Hz, *J* = 7.0 Hz, 1H), 2.82 (s, 3H), 0.03 (s, 9H). ¹³C NMR (101 MHz, benzene-*d₆*) δ 151.41, 147.72, 143.22, 128.31, 127.18, 126.80, 126.10, 102.48, 93.41, 89.11, 55.86, 54.66, -0.56. HRMS m/z: [M+Na]⁺ anal. calcd for C₂₁H₂₆O₃SiNa 377.15489, found 377.15451.

((1-((3S,4R)-4-methoxy-2,2-diphenyloxetan-3-yl)vinyl)oxy)trimethylsilane (*trans*-7).
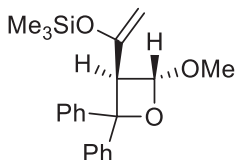
¹H NMR (400 MHz, benzene-*d₆*) δ 7.70-7.66 (m, 2H), 7.64-7.60 (m, 2H), 7.21-7.18 (m, 1H), 7.14-7.09 (m, 3H), 7.05-6.97 (m, 2H), 5.80 (d, *J* = 4.9 Hz, 1H), 4.29 (d, *J* = 4.8 Hz, 1H), 4.12 (d, *J* = 1.6 Hz, 1H), 3.99 (d, *J* = 1.9 Hz, 1H), 3.23 (s, 3H), 0.06 (s, 9H). ¹³C NMR (101 MHz,

benzene-d_6) δ 153.20, 147.70, 143.13, 128.31, 126.76, 126.63, 126.56, 125.43, 102.17, 91.28, 84.63, 58.45, 53.69, -0.85. HRMS m/z: [M+Na]$^+$ anal. calcd for $C_{21}H_{26}O_3SiNa$ 377.15489, found 377.15405.

((1-((3S,4S)-4-methoxy-2,2-diphenyloxetan-3-yl)vinyl)oxy)trimethylsilane (*cis*-7).
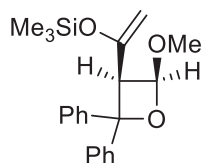
^{1}H NMR (400 MHz, benzene-d_6) δ 7.78-7.77 (m, 2H), 7.77-7.74 (m, 2H), 7.26-7.21 (m, 2H), 7.13-7.06 (m, 2H), 7.04-6.99 (m, 2H), 5.22 (d, J = 6.4 Hz, 1H), 4.89 (t, J = 1.0 Hz, 1H), 4.29 (dd, J = 0.6 Hz, J = 6.5 Hz, 1H), 4.16 (d, J = 1.1 Hz, 1H), 3.23 (s, 3H), 0.02 (s, 9H). ^{13}C NMR (101 MHz, benzene-d_6) δ 151.41, 147.72, 143.22, 128.31, 127.18, 126.80, 126.10, 102.48, 93.41, 89.11, 55.86, 54.66, -0.56. HRMS m/z: [M+Na]$^+$ anal. calcd for $C_{21}H_{26}O_3SiNa$ 377.15489, found 377.15424.

Determination of quantum yields of oxetane formations

I. Number of photon measurement

Preparation:

Potassium ferric oxalate solution:

177.7 mg of potassium ferric oxalate was added to the 20 mL of 0.05 M sulfuric acid solution.

Buffered phenanthroline solution:

2.25 g sodium acetate trihydrate and 10.1 mg of phenanthroline were mixed with 10 mL of 0.5 M sulfuric acid solution.

Procedure:

3 mL of the 0.013 M potassium ferrioxalate solution was irradiated under an LED lamp (365 nm) (Figure 25). After 0.5s, 0.7s, 0.9s of irradiation, 0.5 mL of buffered phenanthroline (0.1%) was added, and the mixture was measured by UV-Vis spectroscopy.

$$Nh\frac{v}{t} = \frac{moles\ Fe^{2+}}{\Phi \times t \times F} = \frac{V_1 \times V_3 \times \Delta A\ (510\ nm)}{10^3 \times V_2 \times l \times \varepsilon(510\ nm) \times \Phi \times t \times F}$$

V_1: the radiated volume (3 mL)

V_2: the aliquot of the irradiated solution taken for the determination of the ferrous ions (3 mL)

V_3: the final volume after phenanthroline was added (3.5 mL)

$\varepsilon = 11100 \ M^{-1}cm^{-1}$

$\phi_{365 \ nm} = 1.21$

F: the mean fraction of light absorbed by the ferrioxalate solution
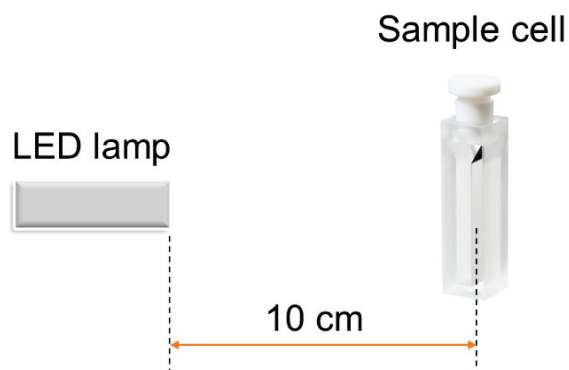
Figure 24. Equipment set-up for the quantum yield measurement
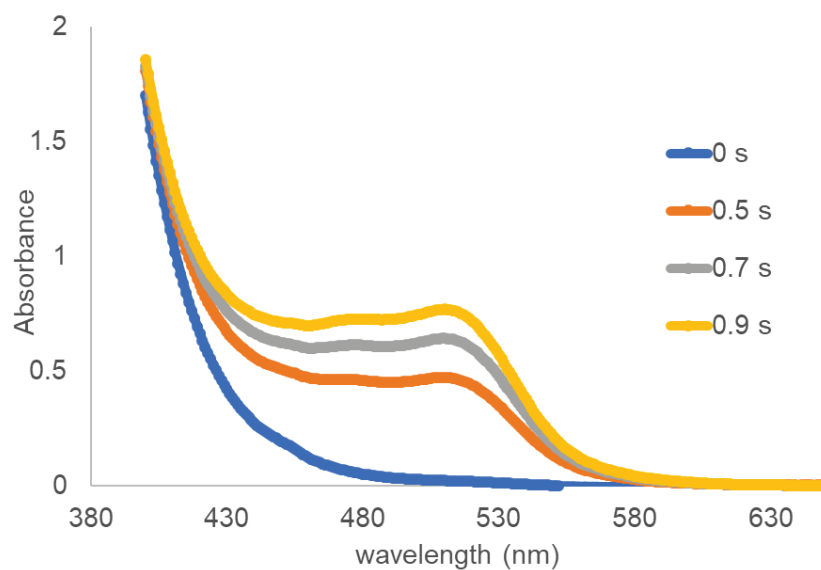
Figure 25. UV spectrum of potassium ferric oxalate solution mixed with phenanthroline after irradiation
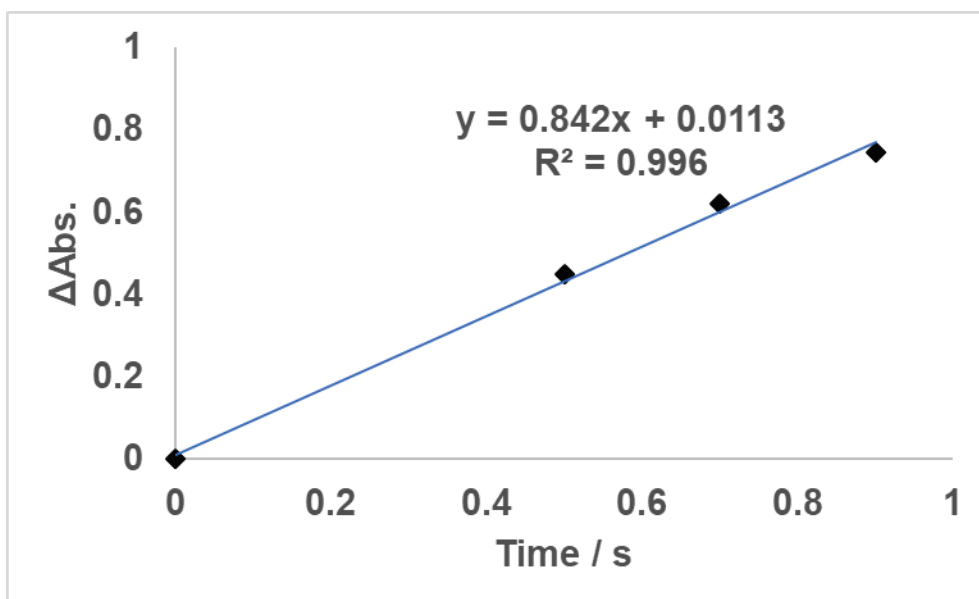
Figure 26. The relative plot of absorption and irradiation of potassium ferric oxalate solution mixed with phenanthroline using LED 365 nm lamp

Table 3 Δ Absorbance value in different time of irradiation

Time of irradiation (s)	Absorbance at 510 nm	Δ Absorbance
0	0.022511	0
0.5	0.471014	0.448503
0.7	0.641684	0.619173
0.9	0.768232	0.745721

$$I = \frac{V_1 \; x \; V_3 \; x \; \Delta A \; (510 \; nm)}{10^3 \; x \; V_2 \; x \; l \; x \; \varepsilon \; (510 \; nm) x \; \phi \; x \; t \; x \; F}$$

- Number of photon in 0.5 s irradiation

$$I = \frac{3 \; x \; 3.5 \; x \; 0.448503}{10^3 \; x \; 3 \; x \; 1 \; x \; 11100 \; x \; 1.21 \; x \; 0.5}$$

$$= 2.33752 \; x \; 10^{-7} \; mol/s$$

- Number of photon in 0.7 s irradiation

$$I = \frac{3 \; x \; 3.5 \; x \; 0.619173}{10^3 \; x \; 3 \; x \; 1 \; x \; 11100 \; x \; 1.21 \; x \; 0.7}$$

$$= 2.30501 \; x \; 10^{-7} \; mol/s$$

- Number of photon in 0.9 s irradiation

$$I = \frac{3 \ x \ 3.5 \ x \ 0.745721}{10^3 \ x \ 3 \ x \ 1 \ x \ 11100 \ x \ 1.21 \ x \ 0.9}$$

$$= 2.1592 \ x \ 10^{-7} \text{ mol/s}$$

Average number of photon

$$I = \frac{2.33752 \ x \ 10^{-7} + \ 2.30501 \ x \ 10^{-7} + \ 2.1592 \ x \ 10^{-7}}{3}$$

$$= 2.26725 \text{ x } 10^{-7} \text{ mol/s}$$

$$= 2.26725 \text{ x } 10^{-4} \text{ mmol/s}$$

II. Quantum yield measurement

Procedure:

0.16 M 1a and 0.3 M 2b in 3 mL benzene (20 min N_2 bubbled) was irradiated as the exact same condition of potassium ferric oxalate solution within 5 hours / 18,000 s (chemical yield 1%). The chemical yield of the product was calculated by internal standard triphenylmethane.

Based on the integration of triphenylmethane, mmol of *trans*-5a and *trans*-6a = 0.007108 mmol.

$$\Phi = \frac{moles \ of \ oxetane}{I \ x \ T_{irradiation}} = \frac{0.007108}{2.26725 \ x \ 10^{-4} \ x \ 18000}$$

$$= \textbf{1.7 x 10}^{\textbf{-3}}$$

2.4 Supplementary material
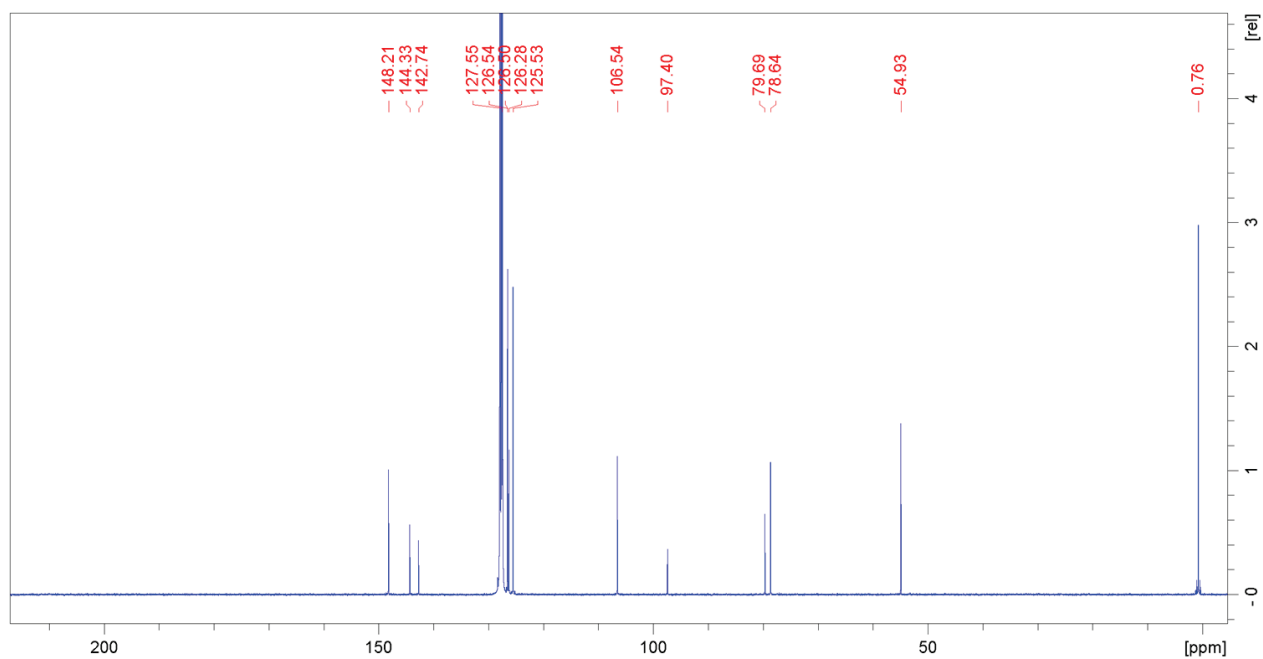
Figure 27. ^{13}C NMR spectrum of *trans*-**5** (101 MHz, C_6D_6)
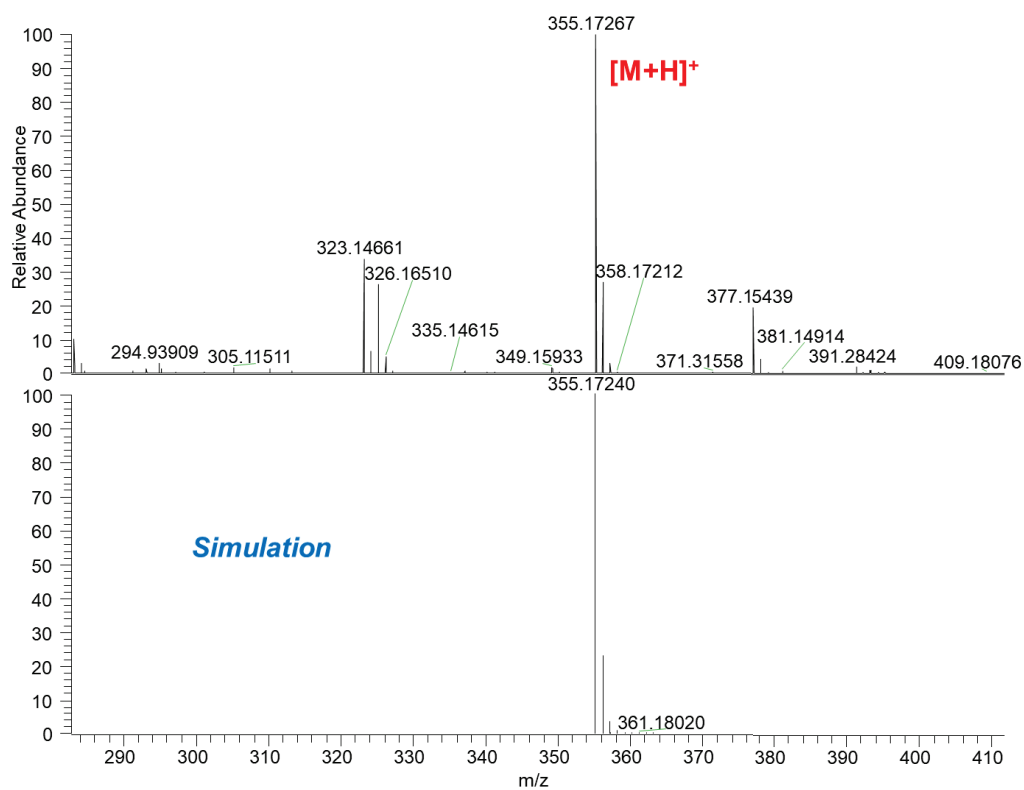
Figure 28. HRMS spectrum of *trans*-**5**
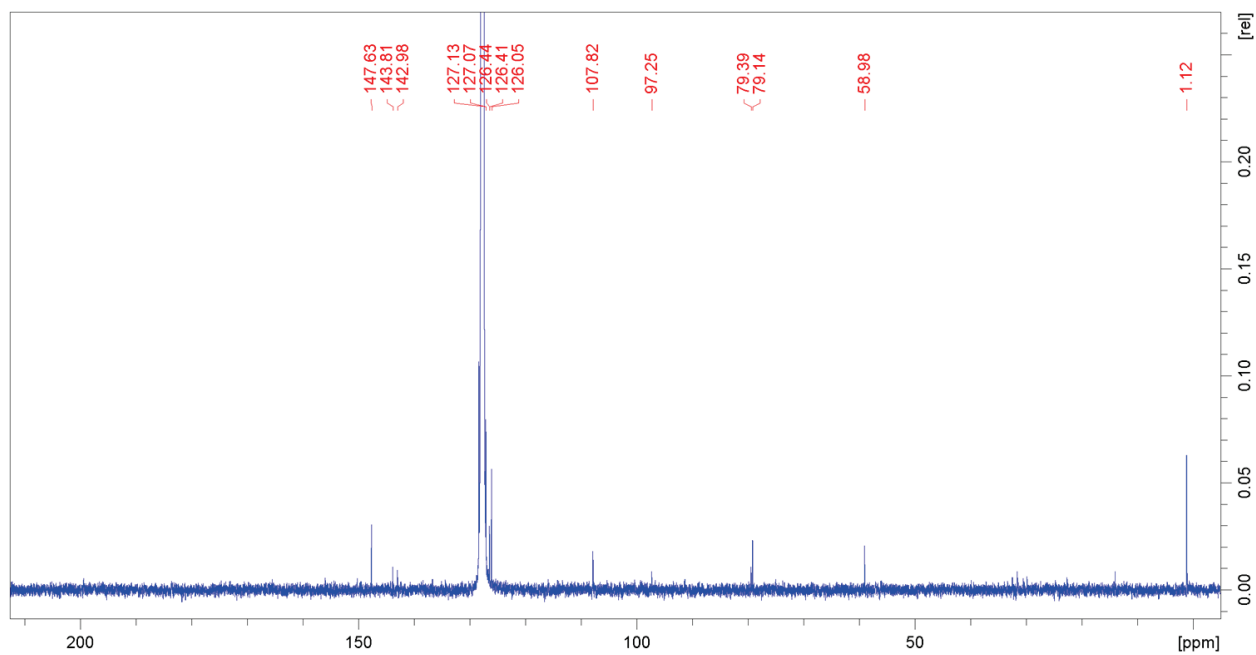
Figure 29. ^{13}C NMR spectrum of *cis*-**5** (101 MHz, C_6D_6)
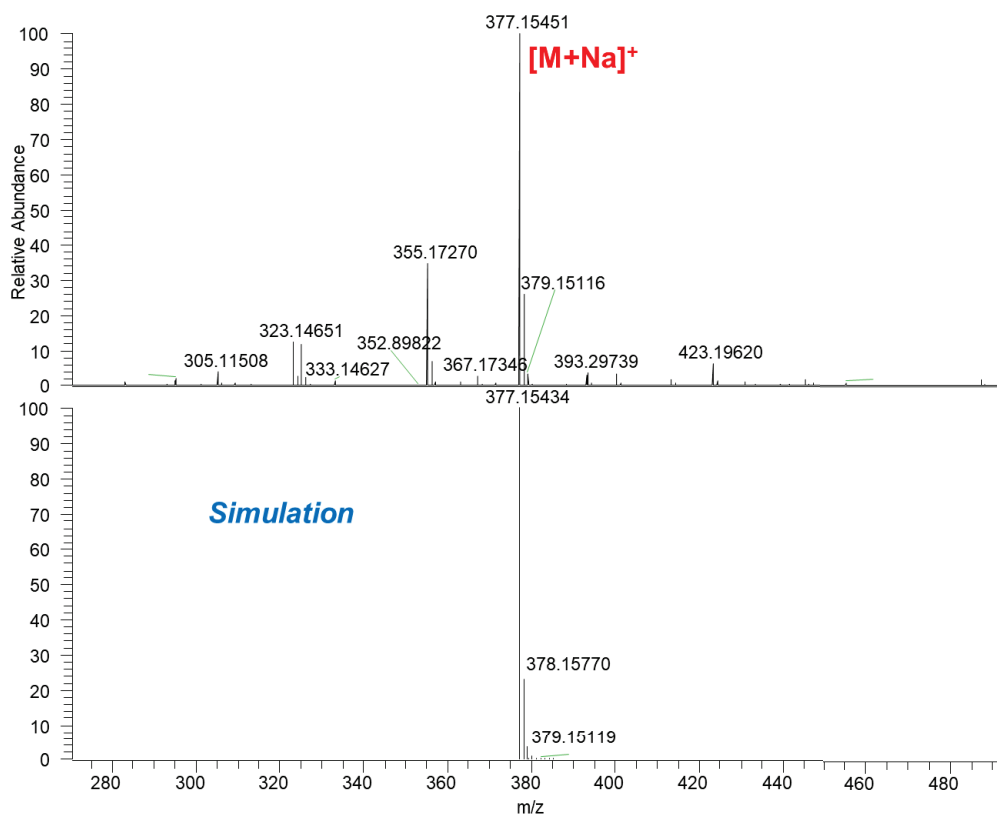
Figure 30. HRMS spectrum of *cis*-**5**

44
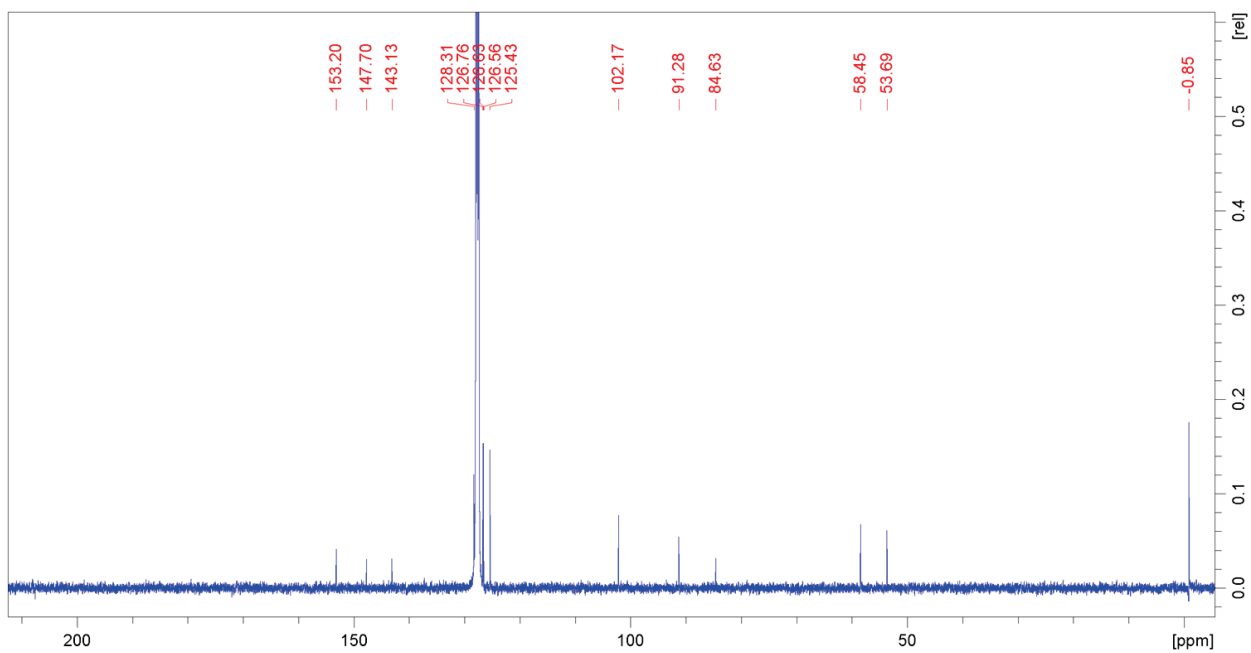
Figure 31. ^{13}C NMR spectrum of *trans*-**7** (101 MHz, C_6D_6)
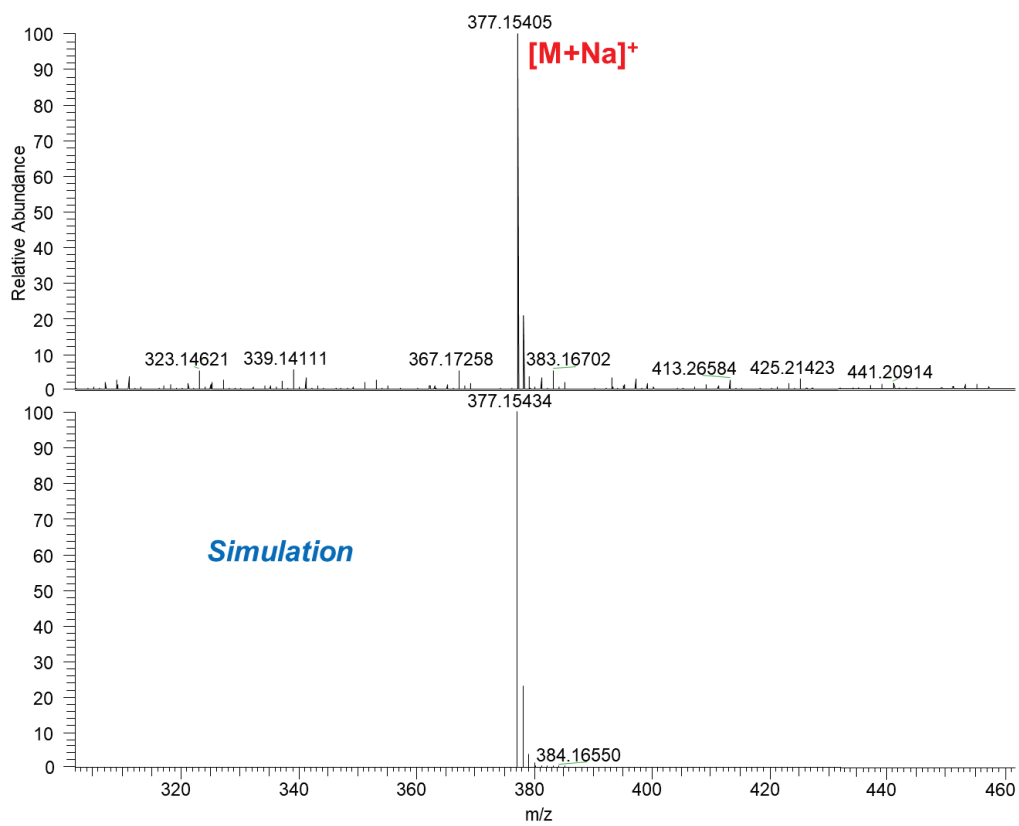
Figure 32. HRMS spectrum of *trans*-**7**

Figure 33. ^{13}C NMR spectrum of *cis*-**7** (101 MHz, C$_6$D$_6$)

Figure 34. HRMS spectrum of *cis*-**7**
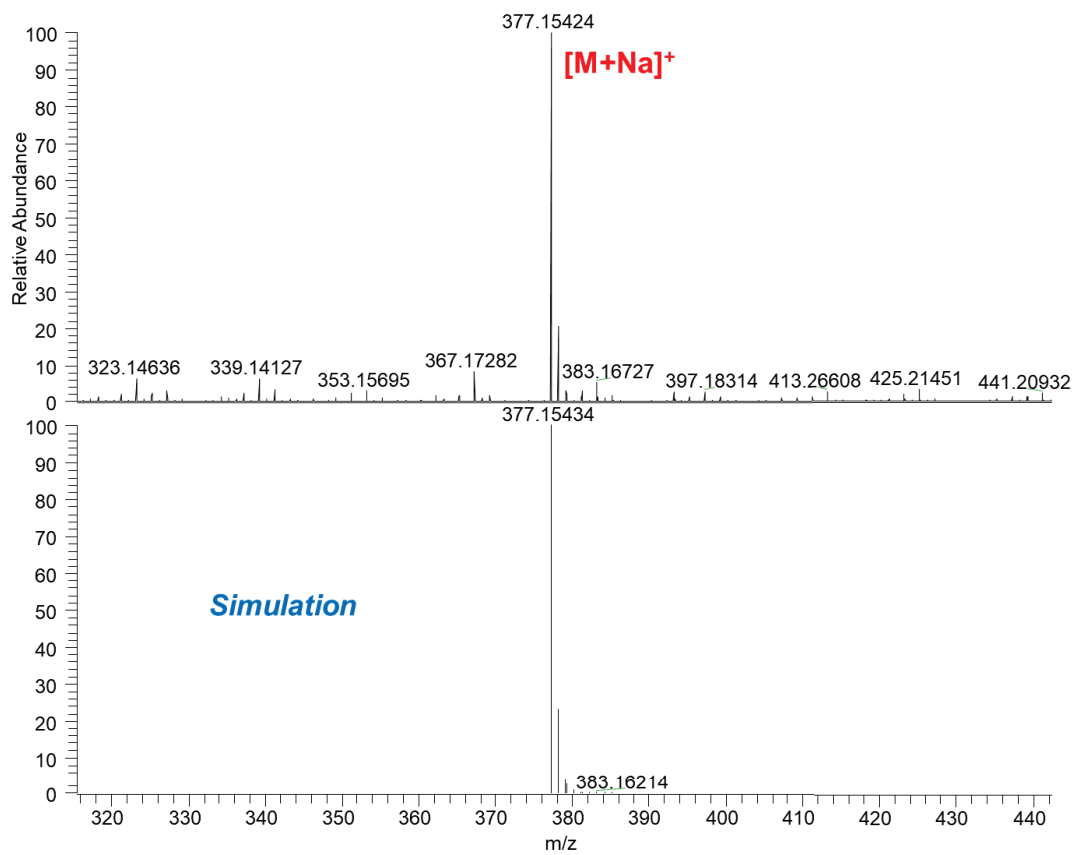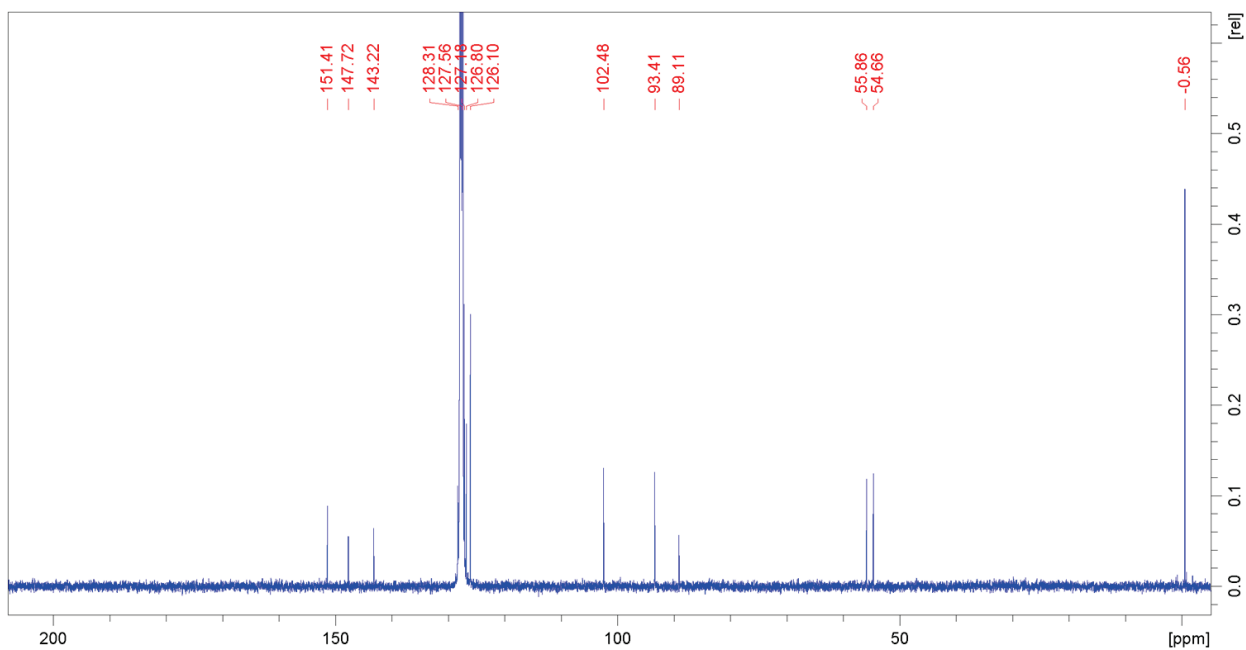
Structure of optimized structures **T-DR1**-gauche-*trans*
```
 Zero-point correction = 0.419254 (Hartree/Particle)
 Thermal correction to Energy = 0.446593
 Thermal correction to Enthalpy = 0.447537
 Thermal correction to Gibbs Free Energy = 0.357594
 Sum of electronic and zero-point Energies = -1330.604995
 Sum of electronic and thermal Energies = -1330.577656
 Sum of electronic and thermal Enthalpies = -1330.576712
 Sum of electronic and thermal Free Energies = -1330.666654
```

Center Number	Atomic Number	Atomic Type	Coordinates (Angstroms)		
			X	Y	Z
1	6	0	0.479579	-0.331342	-1.802880
2	1	0	-0.107521	-1.251459	-1.749213
3	1	0	0.934887	-0.255922	-2.794003
4	6	0	1.530988	-0.307727	-0.741006
5	8	0	1.185497	-0.812434	0.487016
6	14	0	1.268901	-2.413093	1.038258
7	6	0	0.473123	-3.595066	-0.197943
8	1	0	0.991276	-3.586599	-1.164413
9	1	0	-0.580158	-3.349974	-0.375024
10	1	0	0.515608	-4.623307	0.183607
11	6	0	0.322116	-2.388656	2.659914
12	1	0	0.744273	-1.653320	3.354179
13	1	0	0.351066	-3.369267	3.150606
14	1	0	-0.728174	-2.126818	2.490572
15	6	0	3.073798	-2.892536	1.302656
16	1	0	3.546552	-2.268636	2.069875
17	1	0	3.657236	-2.782921	0.381186
18	1	0	3.156368	-3.937764	1.626750
19	6	0	2.739054	0.385067	-0.905701
20	1	0	2.922211	0.781560	-1.900340
21	6	0	3.666200	0.599857	0.092346
22	1	0	3.503012	0.269905	1.110621
23	8	0	4.860254	1.235156	-0.023059
24	6	0	5.222866	1.746418	-1.296648
25	1	0	5.282377	0.945202	-2.045336
26	1	0	6.206594	2.202408	-1.171933
27	1	0	4.508110	2.506240	-1.639401
28	8	0	-0.421581	0.818465	-1.757508
29	6	0	-1.381351	0.862084	-0.773721
30	6	0	-1.435747	2.092206	-0.026544
31	6	0	-1.502158	4.546246	1.391770
32	6	0	-2.600016	2.510196	0.671421
33	6	0	-0.316358	2.965847	-0.010984
34	6	0	-0.353039	4.163554	0.690154
35	6	0	-2.624412	3.710675	1.369738
36	1	0	-3.495076	1.898946	0.632971
37	1	0	0.578409	2.673392	-0.547403
38	1	0	0.523789	4.806556	0.694607
39	1	0	-3.532241	4.006557	1.889751
40	1	0	-1.525888	5.484509	1.939189
41	6	0	-2.325246	-0.240690	-0.680608
42	6	0	-4.125772	-2.423788	-0.540195
43	6	0	-2.905231	-0.635301	0.549182
44	6	0	-2.669541	-0.985115	-1.834965

```
   45              6              0         -3.556083    -2.054572    -1.763251
   46              6              0         -3.792198    -1.706012     0.612967
   47              1              0         -2.630783    -0.108707     1.457499
   48              1              0         -2.252614    -0.687357    -2.792385
   49              1              0         -3.814009    -2.598145    -2.668835
   50              1              0         -4.218562    -1.990094     1.571866
   51              1              0         -4.818152    -3.259261    -0.486401
 ---------------------------------------------------------------------
```

Structure of optimized structures **T-DR1**-anti-*trans*

Zero-point correction = 0.418977 (Hartree/Particle)
Thermal correction to Energy = 0.446474
Thermal correction to Enthalpy = 0.447418
Thermal correction to Gibbs Free Energy = 0.356258
Sum of electronic and zero-point Energies = -1330.604447
Sum of electronic and thermal Energies = -1330.576950
Sum of electronic and thermal Enthalpies = -1330.576006
Sum of electronic and thermal Free Energies = -1330.667166

```
 ---------------------------------------------------------------------
 Center      Atomic      Atomic           Coordinates (Angstroms)
 Number      Number      Type          X            Y            Z
 ---------------------------------------------------------------------
    1           6           0        0.616991    -0.170509    -0.618333
    2           1           0        0.700163    -1.248210    -0.799123
    3           1           0        0.487560     0.318253    -1.591425
    4           6           0        1.912116     0.348069     0.080540
    5           8           0        3.046588     0.015452    -0.717907
    6          14           0        4.054998    -1.210894    -0.164702
    7           6           0        5.482743    -1.458739    -1.389652
    8           1           0        6.056417    -0.533259    -1.493937
    9           1           0        5.093933    -1.742481    -2.371034
   10           1           0        6.153657    -2.247736    -1.037029
   11           6           0        3.168769    -2.863354     0.001012
   12           1           0        2.363130    -2.795728     0.737577
   13           1           0        3.865239    -3.642916     0.324655
   14           1           0        2.735836    -3.163986    -0.957283
   15           6           0        4.829147    -0.773258     1.501384
   16           1           0        4.053405    -0.655787     2.263632
   17           1           0        5.387437     0.164909     1.427138
   18           1           0        5.515393    -1.561465     1.823376
   19           6           0        1.764528     1.823612     0.322625
   20           1           0        0.813418     2.111707     0.765727
   21           6           0        2.688419     2.748717     0.023683
   22           1           0        3.634099     2.459681    -0.409951
   23           8           0        2.640121     4.113542     0.177360
   24           6           0        1.391455     4.613296     0.646185
   25           1           0        0.579131     4.363632    -0.044240
   26           1           0        1.466188     5.703634     0.692116
   27           1           0        1.176508     4.252816     1.658036
   28           8           0       -0.558585     0.056764     0.189176
   29           6           0       -1.813110    -0.282265    -0.457813
   30           6           0       -2.303389    -1.635661    -0.067887
   31           6           0       -3.271918    -4.186548     0.583096
   32           6           0       -2.974593    -2.400925    -1.017146
   33           6           0       -2.111827    -2.159082     1.208199
   34           6           0       -2.591919    -3.429429     1.538702
```

48

```
35          6          0       -3.461730    -3.670817    -0.699298
36          1          0       -3.094158    -1.972379    -2.005559
37          1          0       -1.560237    -1.556983     1.921630
38          1          0       -2.417129    -3.816753     2.534991
39          1          0       -3.976634    -4.246512    -1.458358
40          1          0       -3.639026    -5.174396     0.833434
41          6          0       -2.783286     0.835986    -0.295555
42          6          0       -4.617329     2.943268    -0.085988
43          6          0       -3.327157     1.411722    -1.439143
44          6          0       -3.151687     1.327192     0.953692
45          6          0       -4.067794     2.375681     1.065248
46          6          0       -4.243868     2.461543    -1.341109
47          1          0       -3.000033     1.020619    -2.394341
48          1          0       -2.691210     0.875911     1.825231
49          1          0       -4.333928     2.744198     2.048107
50          1          0       -4.648068     2.897241    -2.246354
51          1          0       -5.323411     3.761446    -0.004882
---------------------------------------------------------------------
```

Structure of optimized structures **T-DR3**-gauche-*trans*

```
 Zero-point correction = 0.417613 (Hartree/Particle)
 Thermal correction to Energy = 0.444952
 Thermal correction to Enthalpy = 0.445896
 Thermal correction to Gibbs Free Energy = 0.356960
 Sum of electronic and zero-point Energies = -1330.595152
 Sum of electronic and thermal Energies = -1330.567813
 Sum of electronic and thermal Enthalpies = -1330.566869
 Sum of electronic and thermal Free Energies = -1330.655805
```

```
---------------------------------------------------------------------
Center      Atomic     Atomic           Coordinates (Angstroms)
Number      Number     Type          X            Y            Z
---------------------------------------------------------------------
    1          6          0       -2.068025    -1.570366    -0.179916
    2          8          0       -2.905597    -1.070245     0.793230
    3         14          0       -4.232692    -0.042772     0.574425
    4          6          0       -5.684572    -0.997498    -0.161553
    5          1          0       -5.452438    -1.385053    -1.160267
    6          1          0       -6.566680    -0.351575    -0.256374
    7          1          0       -5.962800    -1.847659     0.472389
    8          6          0       -3.754056     1.384006    -0.559798
    9          1          0       -3.492881     1.028552    -1.563528
   10          1          0       -2.893630     1.938675    -0.168501
   11          1          0       -4.588365     2.088485    -0.667061
   12          8          0        1.122910    -0.266013    -1.582244
   13          6          0        1.796491     0.421904    -0.595270
   14          6          0        2.933615    -0.239972     0.033382
   15          6          0        5.153199    -1.550743     1.196744
   16          6          0        3.329512     0.033163     1.363600
   17          6          0        3.671650    -1.207418    -0.688680
   18          6          0        4.765993    -1.844201    -0.115313
   19          6          0        4.423263    -0.614139     1.932904
   20          1          0        2.750773     0.730345     1.961026
   21          1          0        3.369106    -1.442801    -1.702178
   22          1          0        5.325265    -2.573175    -0.696287
   23          1          0        4.699107    -0.394446     2.961143
   24          1          0        6.007880    -2.052633     1.641977
   25          6          0        1.437101     1.811408    -0.456161
```

26	6	0	0.683696	4.542398	-0.240532
27	6	0	2.263391	2.758885	0.207693
28	6	0	0.238818	2.300614	-1.045182
29	6	0	-0.127739	3.635006	-0.931547
30	6	0	1.884856	4.090906	0.316874
31	1	0	3.221295	2.447844	0.607614
32	1	0	-0.390228	1.611878	-1.596140
33	1	0	-1.053185	3.974019	-1.390610
34	1	0	2.542049	4.789523	0.828663
35	1	0	0.393161	5.585467	-0.152268
36	8	0	0.910743	-2.567861	-1.003430
37	6	0	1.000490	-3.010442	0.352493
38	1	0	1.377680	-2.233990	1.025070
39	1	0	1.712632	-3.838563	0.338722
40	1	0	0.031945	-3.370695	0.716963
41	6	0	-2.482666	-2.658838	-0.931037
42	1	0	-3.455653	-3.105843	-0.766390
43	1	0	-1.824441	-3.116936	-1.659517
44	6	0	0.229408	-1.369506	-1.289887
45	1	0	-0.216259	-1.537418	-2.274258
46	6	0	-0.813766	-0.961505	-0.289496
47	1	0	-0.574438	-0.157926	0.398164
48	6	0	-4.639284	0.550439	2.309751
49	1	0	-5.523529	1.199336	2.309983
50	1	0	-4.845385	-0.295677	2.975210
51	1	0	-3.805973	1.117418	2.739635

Structure of optimized structures **T-DR3**-anti-*trans*

```
Zero-point correction = 0.417152 (Hartree/Particle)
Thermal correction to Energy = 0.444841
Thermal correction to Enthalpy = 0.445785
Thermal correction to Gibbs Free Energy = 0.353250
Sum of electronic and zero-point Energies = -1330.603665
Sum of electronic and thermal Energies = -1330.575976
Sum of electronic and thermal Enthalpies = -1330.575032
Sum of electronic and thermal Free Energies = -1330.667567
```

Center Number	Atomic Number	Atomic Type	Coordinates (Angstroms) X	Y	Z
1	6	0	2.440748	0.658473	-0.672026
2	8	0	3.765283	0.544850	-1.072796
3	14	0	4.896773	-0.184073	-0.090756
4	6	0	5.049473	-2.037851	-0.326874
5	1	0	4.128014	-2.544194	-0.023610
6	1	0	5.872396	-2.437275	0.274330
7	1	0	5.243373	-2.277624	-1.375684
8	6	0	4.755708	0.271990	1.728924
9	1	0	3.818142	-0.101766	2.149364
10	1	0	4.781501	1.358396	1.855252
11	1	0	5.582617	-0.159965	2.299356

```
  12         8         0      -0.755090   -0.365399   -0.248326
  13         6         0      -2.026994   -0.021849    0.386856
  14         6         0      -2.330947    1.428599    0.246865
  15         6         0      -2.917446    4.163689    0.079785
  16         6         0      -2.713246    2.137706    1.380472
  17         6         0      -2.235060    2.096277   -0.969919
  18         6         0      -2.525514    3.460199   -1.060039
  19         6         0      -3.008963    3.500359    1.304693
  20         1         0      -2.749127    1.592252    2.316674
  21         1         0      -1.893801    1.529820   -1.829636
  22         1         0      -2.420484    3.960933   -2.014427
  23         1         0      -3.289902    4.032153    2.205164
  24         1         0      -3.128016    5.223814    0.017682
  25         6         0      -3.104063   -0.964035   -0.019505
  26         6         0      -5.158647   -2.746499   -0.691423
  27         6         0      -3.906887   -1.519085    0.970745
  28         6         0      -3.325892   -1.313857   -1.347835
  29         6         0      -4.349653   -2.201268   -1.689830
  30         6         0      -4.935195   -2.407116    0.643343
  31         1         0      -3.688381   -1.242560    1.996426
  32         1         0      -2.664590   -0.891600   -2.095886
  33         1         0      -4.493035   -2.465874   -2.730047
  34         1         0      -5.539688   -2.830608    1.435351
  35         1         0      -5.947310   -3.442180   -0.950809
  36         8         0       0.481354   -1.578650    1.483666
  37         6         0       0.228866   -2.790965    0.805663
  38         1         0      -0.743538   -2.789787    0.307914
  39         1         0       0.213385   -3.592988    1.550864
  40         1         0       1.019341   -3.030153    0.089498
  41         6         0       1.832442    1.839849   -0.795313
  42         1         0       2.382956    2.702229   -1.134869
  43         1         0       0.779614    1.936290   -0.561031
  44         6         0       0.444125   -0.452278    0.587596
  45         1         0       0.487962    0.442846    1.216943
  46         6         0       1.714200   -0.581676   -0.285756
  47         1         0       1.381473   -1.084895   -1.206983
  48         6         0       6.650060    0.487654   -0.578984
  49         1         0       7.396331   -0.000052    0.012728
  50         1         0       6.831572    0.290986   -1.614974
  51         1         0       6.689297    1.542517   -0.403985
 ----------------------------------------------------------------
```

Structure of optimized structures **T-DR1**-gauche-*cis*

```
Zero-point correction = 0.418613 (Hartree/Particle)
Thermal correction to Energy = 0.446261
Thermal correction to Enthalpy = 0.447205
Thermal correction to Gibbs Free Energy = 0.356120
Sum of electronic and zero-point Energies = -1330.603339
Sum of electronic and thermal Energies = -1330.575691
Sum of electronic and thermal Enthalpies = -1330.574747
Sum of electronic and thermal Free Energies = -1330.665832


 ----------------------------------------------------------------
 Center     Atomic     Atomic          Coordinates (Angstroms)
 Number     Number      Type         X           Y           Z
 ----------------------------------------------------------------
     1         6         0       0.109654   -0.563440   -1.996549
```

```
     2          1           0       -0.347148    -1.488802    -1.632188
     3          1           0        0.298963    -0.655840    -3.068976
     4          6           0        1.383128    -0.274554    -1.259814
     5          8           0        1.362403    -0.497651     0.084301
     6         14           0        1.796105    -1.863835     0.985357
     7          6           0        1.964261    -1.214836     2.740219
     8          1           0        1.027631    -0.757202     3.078226
     9          1           0        2.747246    -0.450817     2.796055
    10          1           0        2.218949    -2.017908     3.442495
    11          6           0        3.409831    -2.593486     0.341475
    12          1           0        3.315654    -2.915514    -0.702486
    13          1           0        3.702111    -3.470728     0.932327
    14          1           0        4.215738    -1.855323     0.391371
    15          6           0        0.432408    -3.163981     0.879996
    16          1           0        0.324172    -3.558497    -0.137708
    17          1           0       -0.540178    -2.760205     1.182547
    18          1           0        0.662101    -4.014979     1.534520
    19          6           0        2.455710     0.355716    -1.891123
    20          1           0        2.335241     0.523051    -2.958927
    21          6           0        3.651121     0.828418    -1.379575
    22          8           0       -0.861266     0.520126    -1.902098
    23          6           0       -1.637828     0.615569    -0.770681
    24          6           0       -1.614205     1.898678    -0.115866
    25          6           0       -1.530715     4.452615     1.112195
    26          6           0       -2.660184     2.342340     0.736154
    27          6           0       -0.540056     2.796488    -0.353292
    28          6           0       -0.502224     4.043675     0.255319
    29          6           0       -2.610359     3.592312     1.340291
    30          1           0       -3.527406     1.710323     0.892886
    31          1           0        0.260751     2.485227    -1.013401
    32          1           0        0.338695     4.705765     0.063355
    33          1           0       -3.429006     3.906679     1.983092
    34          1           0       -1.496535     5.429586     1.586588
    35          6           0       -2.509280    -0.502181    -0.448149
    36          6           0       -4.182355    -2.716082     0.124952
    37          6           0       -2.894673    -0.806424     0.880228
    38          6           0       -2.978874    -1.355533    -1.476467
    39          6           0       -3.802978    -2.438636    -1.192347
    40          6           0       -3.719830    -1.892696     1.156446
    41          1           0       -2.515827    -0.198617     1.695490
    42          1           0       -2.708769    -1.131545    -2.503859
    43          1           0       -4.160518    -3.067016    -2.004395
    44          1           0       -3.994937    -2.105917     2.186440
    45          1           0       -4.825829    -3.563352     0.344928
    46          1           0        4.383278     1.302362    -2.030625
    47          8           0        4.011395     0.700530    -0.074293
    48          6           0        5.139844     1.472920     0.315160
    49          1           0        4.923795     2.547260     0.251756
    50          1           0        6.013615     1.242712    -0.310356
    51          1           0        5.358121     1.207643     1.351127
    -------------------------------------------------------------------
```

Structure of optimized structures **T-DR1**-anti-*cis*

```
Zero-point correction=                          0.418064 (Hartree/Particle)
Thermal correction to Energy=                   0.445949
Thermal correction to Enthalpy=                 0.446893
```

```
Thermal correction to Gibbs Free Energy=              0.354674
Sum of electronic and zero-point Energies=            -1330.604102
Sum of electronic and thermal Energies=               -1330.576217
Sum of electronic and thermal Enthalpies=             -1330.575273
Sum of electronic and thermal Free Energies=          -1330.667492


---------------------------------------------------------------------
Center     Atomic      Atomic            Coordinates (Angstroms)
Number     Number       Type         X           Y           Z
---------------------------------------------------------------------
   1          6           0       -0.546064   -0.324205   -0.606928
   2          1           0       -0.632743    0.688924   -1.013961
   3          1           0       -0.420070   -1.006410   -1.453762
   4          6           0       -1.820459   -0.672451    0.197312
   5          8           0       -3.033015   -0.295050   -0.418747
   6         14           0       -3.806511    1.085068    0.147765
   7          6           0       -5.404471    1.363638   -0.836221
   8          1           0       -6.068427    0.501405   -0.730687
   9          1           0       -5.175662    1.501344   -1.897309
  10          1           0       -5.925904    2.253664   -0.471883
  11          6           0       -2.757410    2.638163   -0.038857
  12          1           0       -1.843204    2.558802    0.556690
  13          1           0       -3.311568    3.518426    0.297826
  14          1           0       -2.475335    2.785781   -1.084862
  15          6           0       -4.301251    0.908949    1.962922
  16          1           0       -3.413547    0.788700    2.590089
  17          1           0       -4.944477    0.035236    2.098531
  18          1           0       -4.845485    1.797219    2.298415
  19          6           0       -1.787425   -1.962527    0.927193
  20          1           0       -1.240836   -1.874506    1.867312
  21          6           0       -2.271635   -3.185498    0.662543
  22          8           0        0.640610   -0.386283    0.213999
  23          6           0        1.866467    0.012651   -0.460697
  24          6           0        2.152778    1.469862   -0.300572
  25          6           0        2.735950    4.205459   -0.080393
  26          6           0        2.809144    2.138474   -1.330012
  27          6           0        1.781157    2.182662    0.836533
  28          6           0        2.069070    3.545371    0.952332
  29          6           0        3.106054    3.499683   -1.226573
  30          1           0        3.070131    1.561182   -2.209095
  31          1           0        1.241680    1.649365    1.611687
  32          1           0        1.755260    4.076513    1.841762
  33          1           0        3.613573    3.995382   -2.043893
  34          1           0        2.954463    5.262546    0.002059
  35          6           0        2.971989   -0.908704   -0.074358
  36          6           0        5.070822   -2.652299    0.557200
  37          6           0        3.640007   -1.599417   -1.080243
  38          6           0        3.350530   -1.101611    1.249816
  39          6           0        4.397917   -1.968662    1.572198
  40          6           0        4.688580   -2.469389   -0.772662
  41          1           0        3.302739   -1.440289   -2.097630
  42          1           0        2.795141   -0.569299    2.013235
  43          1           0        4.668782   -2.108957    2.611287
  44          1           0        5.188618   -3.000948   -1.572422
  45          1           0        5.878532   -3.332324    0.803119
  46          1           0       -2.131035   -3.963484    1.402134
  47          8           0       -2.920855   -3.745039   -0.401718
  48          6           0       -2.961947   -2.963705   -1.586407
```

53

```
   49          1          0       -1.991247    -2.540076    -1.846314
   50          1          0       -3.754984    -2.217835    -1.529159
   51          1          0       -3.235981    -3.638990    -2.404919
   ------------------------------------------------------------------
```

Structure of optimized structures **T-DR3**-gauche-*cis*

```
 Zero-point correction = 0.417392 (Hartree/Particle)
 Thermal correction to Energy = 0.444784
 Thermal correction to Enthalpy = 0.445728
 Thermal correction to Gibbs Free Energy = 0.355511
 Sum of electronic and zero-point Energies = -1330.595087
 Sum of electronic and thermal Energies = -1330.567695
 Sum of electronic and thermal Enthalpies = -1330.566751
 Sum of electronic and thermal Free Energies = -1330.656968
```

```
 ---------------------------------------------------------------------
 Center     Atomic     Atomic            Coordinates (Angstroms)
 Number     Number     Type        X            Y            Z
 ---------------------------------------------------------------------
    1          6          0       1.523080    -0.390309    -0.109331
    2          8          0       2.367627     0.501447    -0.744855
    3         14          0       4.051052     0.566890    -0.635873
    4          6          0       4.818284    -1.030113    -1.284413
    5          1          0       4.474162    -1.903959    -0.719181
    6          1          0       5.912246    -0.994944    -1.205584
    7          1          0       4.566134    -1.195262    -2.338455
    8          6          0       4.568072     0.839606     1.158895
    9          1          0       4.206482     0.035104     1.810103
   10          1          0       4.174390     1.785199     1.549536
   11          1          0       5.661083     0.870934     1.249654
   12          8          0      -1.380671    -0.104065     1.824671
   13          6          0      -1.917513     0.131889     0.570447
   14          6          0      -2.251009    -1.012644    -0.265744
   15          6          0      -2.933287    -3.247149    -1.859213
   16          6          0      -2.222061    -0.940222    -1.678252
   17          6          0      -2.610231    -2.247204     0.323263
   18          6          0      -2.950868    -3.341451    -0.463738
   19          6          0      -2.560046    -2.041553    -2.459194
   20          1          0      -1.894000    -0.023972    -2.157835
   21          1          0      -2.619430    -2.326235     1.403580
   22          1          0      -3.237514    -4.275132     0.013806
   23          1          0      -2.518035    -1.962113    -3.542567
   24          1          0      -3.199017    -4.105201    -2.470815
   25          6          0      -2.265188     1.505398     0.311858
   26          6          0      -2.937896     4.228404    -0.131434
   27          6          0      -3.179323     1.886599    -0.707646
   28          6          0      -1.734291     2.543178     1.124426
   29          6          0      -2.060694     3.873431     0.899449
   30          6          0      -3.498596     3.220775    -0.923961
   31          1          0      -3.660663     1.122654    -1.307137
   32          1          0      -1.065921     2.280305     1.935493
   33          1          0      -1.629812     4.643645     1.534514
   34          1          0      -4.204767     3.477812    -1.709588
   35          1          0      -3.190888     5.270580    -0.305188
   36          8          0      -0.082979    -2.017118     1.902809
   37          6          0       0.978875    -2.654111     2.595322
```

```
38            1            0         1.950469    -2.467234     2.118611
39            1            0         0.768341    -3.725657     2.569813
40            1            0         1.025226    -2.321744     3.643821
41            6            0         1.288421    -1.610276    -0.727230
42            1            0         1.761074    -1.832262    -1.676807
43            1            0         0.596576    -2.321651    -0.299981
44            6            0        -0.046582    -0.609638     1.982277
45            1            0         0.184209    -0.328856     3.022170
46            6            0         0.950805     0.067030     1.082033
47            1            0         1.213101     1.077748     1.380765
48            6            0         4.524982     2.031982    -1.711616
49            1            0         5.611452     2.181872    -1.721925
50            1            0         4.197220     1.882714    -2.746605
51            1            0         4.061731     2.955347    -1.346162
    ----------------------------------------------------------------
```

Structure of optimized structures **T-DR3**-anti-*cis*
```
 Zero-point correction = 0.417330 (Hartree/Particle)
 Thermal correction to Energy = 0.444833
 Thermal correction to Enthalpy = 0.445777
 Thermal correction to Gibbs Free Energy = 0.354438
 Sum of electronic and zero-point Energies = -1330.601788
 Sum of electronic and thermal Energies = -1330.574284
 Sum of electronic and thermal Enthalpies = -1330.573340
 Sum of electronic and thermal Free Energies = -1330.664680
```

```
    ----------------------------------------------------------------
 Center      Atomic      Atomic          Coordinates (Angstroms)
 Number      Number      Type         X           Y            Z
    ----------------------------------------------------------------
    1            6            0         2.371129    -0.622961    -0.347060
    2            8            0         3.514119    -0.197896    -0.996472
    3           14            0         5.033935     0.075702    -0.311962
    4            6            0         5.709642    -1.506571     0.462090
    5            1            0         5.051470    -1.886801     1.251760
    6            1            0         6.695285    -1.327699     0.910188
    7            1            0         5.824391    -2.299316    -0.286410
    8            6            0         4.907863     1.427953     0.998441
    9            1            0         4.205895     1.154307     1.795026
   10            1            0         4.563994     2.373584     0.563354
   11            1            0         5.882745     1.611682     1.467109
   12            8            0        -0.794142    -0.215875    -0.441876
   13            6            0        -2.144862     0.036481    -0.265714
   14            6            0        -2.553272     1.426978    -0.184900
   15            6            0        -3.283859     4.158178    -0.023535
   16            6            0        -3.711277     1.836051     0.520584
   17            6            0        -1.765042     2.436271    -0.792204
   18            6            0        -2.129324     3.775620    -0.713967
   19            6            0        -4.067794     3.178395     0.593899
   20            1            0        -4.308790     1.092852     1.038163
   21            1            0        -0.881712     2.143625    -1.351119
   22            1            0        -1.514375     4.527062    -1.202905
   23            1            0        -4.957046     3.464953     1.149654
   24            1            0        -3.566280     5.205534     0.036550
   25            6            0        -3.005042    -1.116435    -0.325910
   26            6            0        -4.649702    -3.418683    -0.474331
   27            6            0        -4.380885    -1.018905    -0.663613
   28            6            0        -2.478004    -2.413694    -0.093248
```

55

```
29          6          0          -3.290413    -3.537486    -0.162747
30          6          0          -5.183632    -2.150850    -0.728733
31          1          0          -4.804627    -0.051289    -0.909049
32          1          0          -1.429357    -2.509854     0.158615
33          1          0          -2.862443    -4.518102     0.030445
34          1          0          -6.232009    -2.046382    -0.996873
35          1          0          -5.280926    -4.301417    -0.528101
36          8          0          -0.000500    -0.816920     1.596880
37          6          0           0.566176    -0.442617     2.841502
38          1          0           1.654733    -0.308933     2.772817
39          1          0           0.348364    -1.254102     3.539575
40          1          0           0.118108     0.487927     3.222392
41          6          0           2.195030    -1.984391    -0.154345
42          1          0           2.936660    -2.685429    -0.518726
43          1          0           1.307429    -2.357924     0.336527
44          6          0           0.094083     0.185521     0.600041
45          1          0          -0.250070     1.139206     1.027042
46          6          0           1.463447     0.377765     0.012190
47          1          0           1.727349     1.397093    -0.253062
48          6          0           6.098194     0.625679    -1.758917
49          1          0           7.125206     0.836745    -1.436792
50          1          0           6.142081    -0.150037    -2.531753
51          1          0           5.698295     1.534629    -2.222355
-------------------------------------------------------------------------
```

Table 4. T-DR1-*trans* dihedral angle scan

UB3LYP/6-31G(d) level of theory in the GAUSSIAN 09	
Scan of Total Energy	
X-Axis: Scan Coordinate Dihedral Angle, θ (°)	
Y-Axis: Total Energy (kJ/mol)	
X	**Y**
0	22.72934733
10	24.19710685
20	24.66087517
30	24.03246174
40	23.06073794
50	21.7296882
60	20.2919644
70	16.83583497
80	14.89209855
90	13.66354834
100	11.54526868
110	8.13421908
120	5.004386785
130	2.377574035
140	0.78722992
150	0
160	0.218835425

170	0.73219944
180	1.67795705
190	3.323436666
240	6.588245915
250	6.994699571
260	7.74007902
270	8.729603715
280	8.81716414
290	7.59158074
300	7.47264559
310	7.921474815
320	9.754913975
330	12.53248294
340	15.24669858
350	17.7496665
360	20.40835282

Table 5. T-DR3-*trans* dihedral angle scan

UB3LYP/6-31G(d) level of theory in the GAUSSIAN 09
Scan of Total Energy
X-Axis: Scan Coordinate Dihedral Angle, θ (°)
Y-Axis: Total Energy (kJ/mol)

X	Y
0	42.60275452
10	42.00863012
20	41.35023349
30	40.09676728
40	38.88701564
50	38.24130017
60	37.61110141
70	38.32190302
80	39.88696357
90	41.81163886
100	43.21292071
110	43.29515138
120	42.15820486
130	38.94117971
140	34.24389766
150	29.31352372
160	24.4509927
170	20.32887893
180	17.55330535
190	16.052307
200	16.0066233
210	16.17686072

X	Y
220	15.46259344
230	15.53201167
240	17.9972774
250	22.52894291
260	24.50547182
270	25.73102897
280	27.47732778
290	29.79199484
300	32.28871406
310	34.79777314
320	37.54567395
330	40.06421108
340	41.40662923
350	41.8029222
360	42.09246234

Table 6. T-DR1-*cis* dihedral angle scan

UB3LYP/6-31G(d) level of theory in the GAUSSIAN 09

Scan of Total Energy

X-Axis: Scan Coordinate Dihedral Angle, θ (°)

Y-Axis: Total Energy (kJ/mol)

X	Y
0	19.83707027
10	20.67951446
20	20.40864162
30	19.28083184
40	17.71054655
50	15.7535251
60	13.92008594
70	12.5057816
80	11.97099351
90	11.44691745
100	10.51160933
110	9.591607875
120	8.77961949
130	7.14120247
140	5.37817922
150	4.33538313
160	3.7324108
170	3.10034793
180	2.356412505
190	1.684862115
200	0.64224981
210	0.15275159
220	0

230	0.129305875
240	0.888968045
250	1.62334665
260	2.62114167
270	2.53759826
280	2.472092035
290	2.68714674
300	3.405352265
310	5.50189278
320	8.44702115
330	11.90288804
340	15.28988806
350	17.90845674
360	19.83709653

Table 7. T-DR3-*cis* dihedral angle scan

UB3LYP/6-31G(d) level of theory in the GAUSSIAN 09

Scan of Total Energy

X-Axis: Scan Coordinate Dihedral Angle, θ (°)

Y-Axis: Total Energy (kJ/mol)

X	Y
0	30.60832
10	28.65342
20	27.50025
30	27.37115
40	28.35816
50	30.37522
60	32.618
80	35.02317
90	36.49962
100	37.17797
110	36.64358
120	34.43779
130	30.75639
140	26.45233
150	21.71186
160	17.36574
170	14.07935
180	11.74024

190	10.50271
200	9.839429
210	10.04143
220	11.24
230	13.66877
240	16.71511
250	20.27469
260	23.32321
270	26.27262
280	29.26343
290	31.94824
300	34.41996
310	36.1989
320	37.15337
330	37.19777
340	36.33647
350	34.54819
360	32.80439

Table 8. T-DR1-*trans* bond formation scan

UB3LYP/6-31G(d) level of theory in the GAUSSIAN 09

Scan of Total Energy

X-Axis: Scan Coordinate Distance, r (pm)

Y-Axis: Total Energy (kJ/mol)

X	Y
431.66	94.83911965
421.66	94.73457487
411.66	94.68964206
401.66	94.48555407
391.66	94.10808331
381.66	93.69672522
371.66	93.25396878
361.66	92.79040787
351.66	92.31640798
341.66	91.84267851
331.66	91.36519721
321.66	90.86649923
311.66	90.36345081
301.66	89.82880186
291.66	89.21917127
281.66	88.61108184
271.66	88.1197799
261.66	87.78723407
251.66	87.57450031

241.66	87.41321584
231.66	87.26696761
221.66	86.78085104
211.66	85.18995294
201.66	81.03631742
191.66	72.54330539
181.66	59.15795504
171.66	41.80263602
161.66	22.72626499
151.66	6.671765696
141.66	2.372160254

Table 9. T-DR3-*trans* bond formation scan

UB3LYP/6-31G(d) level of theory in the GAUSSIAN 09

Scan of Total Energy

X-Axis: Scan Coordinate Distance, r (pm)

Y-Axis: Total Energy (kJ/mol)

X	Y
436.00	91.71555968
426.00	91.29974612
416.00	90.9935183
406.00	90.8121225
396.00	90.74536654
386.00	90.76263708
376.00	90.84609385
366.00	91.04492296
356.00	91.0538024
346.00	91.31585093
336.00	91.71102807
326.00	92.26652085
316.00	93.05316004
306.00	94.11975103
296.00	92.19669306
286.00	90.16614448
276.00	89.12260275
266.00	88.23278142
256.00	87.59843699
246.00	87.2741326
236.00	87.20945079
226.00	87.12181685
216.00	86.18140475
206.00	82.67361598
196.00	67.60386297
186.00	60.45608625
176.00	48.51805853
166.00	33.84790137

156.00	19.10113737
146.00	0

Table 10. T-DR1-*cis* bond formation scan

UB3LYP/6-31G(d) level of theory in the GAUSSIAN 09	
Scan of Total Energy	
X-Axis: Scan Coordinate Distance, r (pm)	
Y-Axis: Total Energy (kJ/mol)	

X	Y
441.66	91.80128
431.66	91.62197
421.66	91.47163
411.66	91.33062
401.66	91.01882
391.66	90.61638
381.66	90.17145
371.66	89.71888
361.66	89.255
351.66	88.77541
341.66	88.26299
331.66	87.69377
321.66	87.10895
311.66	86.52237
301.66	85.93275
291.66	85.32465
281.66	84.71787
271.66	84.21895
261.66	83.80736
251.66	83.53622
241.66	83.25738
231.66	82.95645
221.66	82.28549
211.66	80.38282
201.66	75.77755
191.66	66.84509
181.66	53.14716
171.66	35.46947
161.66	16.12274
151.66	0

Table 11. T-DR3-*cis* bond formation scan

UB3LYP/6-31G(d) level of theory in the GAUSSIAN 09
Scan of Total Energy
X-Axis: Scan Coordinate Distance, r (pm)
Y-Axis: Total Energy (kJ/mol)

X	Y
445.99	88.20608
435.99	88.35504
425.99	88.48308
415.99	88.58576
405.99	88.9208
395.99	87.37095
385.99	87.21074
375.99	87.06594
365.99	86.91682
355.99	86.73154
345.99	86.48192
335.99	86.05296
325.99	85.51741
315.99	84.83917
305.99	83.66277
295.99	82.47867
285.99	81.30181
275.99	80.21986
265.99	79.34357
255.99	78.82934
245.99	78.82692
235.99	79.29429
225.99	79.87972
215.99	79.6892
205.99	76.87486
195.99	61.36453
185.99	55.92532
175.99	45.39037
165.99	31.67176
155.99	17.63581

2.5 References

1   S. Danishefsky and T. Kitahara, *J. Am. Chem. Soc.*, 1974, **96**, 7807–7808.

2   E. J. Corey, C. L. Cywin and T. D. Roper, *Tetrahedron Lett.*, 1992, **33**, 6907–6910.

3   Y. Yamashita, H. Ishitani, H. Shimizu and S. Kobayashi, *J. Am. Chem. Soc.*, 2002, **124**, 3292–3302.

4   Y. Yamashita, S. Saito, H. Ishitani and S. Kobayashi, *J. Am. Chem. Soc.*, 2003, **125**, 3793–3798.

5   M. Abe, Y. Shirodai and M. Nojima, *J. Chem. Soc. - Perkin Trans. 1*, 1998, 3253–3260.

6   M. Abe, K. Fujimoto and M. Nojima, *J. Am. Chem. Soc.*, 2000, **122**, 4005–4010.

7   D. A. Pangaribowo and M. Abe, *Org. Biomol. Chem.*, , DOI:10.1039/d0ob00921k.

8   M. W. Wolf, R. E. Brown and L. A. Singer, *J. Am. Chem. Soc.*, 1977, **99**, 526–531.

9   R. A. Marcus and N. Sutin, *Biochim. Biophys. Acta*, 1985, **811**, 265.

10   M. Abe, T. Kawakami, S. Ohata, K. Nozaki and M. Nojima, *J. Am. Chem. Soc.*, 2004, **126**, 2838–2846.

11   A. G. Griesbeck, M. Abe and S. Bondock, *Acc. Chem. Res.*, 2004, **37**, 919–928.

12   P. C. Hariharan and J. A. Pople, *Theor. Chim. Acta*, 1973, **28**, 213–222.

13   C. Lee, W. Yang and R. G. Parr, *Phys. Rev. B*, 1988, **37**, 785–789.

14   A. D. Becke, *J. Chem. Phys.*, 1993, **98**, 5648–5652.

15   M. J. Frisch, G. W. Trucks, H. B. Schlegel, G. E. Scuseria, M. A. Robb, J. R. Cheeseman, G. Scalmani, V. Barone, B. Mennucci, G. A. Petersson, H. Nakatsuji, M. Caricato, X. Li, H. P. Hratchian, A. F. Izmaylov, J. Bloino, G. Zheng, J. L. Sonnenberg, M. Hada, M. Ehara, K. Toyota, R. Fukuda, J. Hasegawa, M. Ishida, T. Nakajima, Y. Honda, O. Kitao, H. Nakai, T. Vreven, J. A. Montgomery, J. Peralta, J. E., F. Ogliaro, M. Bearpark, J. J. Heyd, E. Brothers, K. N. Kudin, V. N. Staroverov, T. Keith, R. Kobayashi, J. Normand, K. Raghavachari, A. Rendell, J. C. Burant, S. S. Iyengar, J. Tomasi, M. Cossi, N. Rega, J. M. Millam, M. Klene, J. E. Knox, J. B. Cross, V. Bakken, C. Adamo, J. Jaramillo, R. Gomperts, R. E. Stratmann, O. Yazyev, A. J. Austin, R. Cammi, C. Pomelli, J. W. Ochterski, R. L. Martin, K. Morokuma, V. G. Zakrzewski, G. A. Voth, P. Salvador, J. J. Dannenberg, S. Dapprich, A. D. Daniels, O. Farkas, J. B. Foresman, J. V. Ortiz, J. Cioslowski and D. J. Fox, *Gaussian 09, Revision D.01,* Gaussian, Inc., Wallingford CT, 2013.

Chapter 3

Summary

Photochemical reactions occur all around us, being an essential aspect of many of the chemical processes occurring in living systems and in the environment. The capability and versatility of photochemistry are increasingly becoming important in improving the quality of our lives through health care, energy production, and the search for solutions to some of the problems of the modernized world. Many industrial and technological processes depend on applications of photochemistry. The development of many new devices has been made possible by the result of photochemical research.

When a molecule absorbs light, it can reach an electronically excited state. As a result, the distribution of electrons in the molecule is significantly different from that in the ground state. The chemical property and reactivity of the excited state also change. The photochemical reactions may substantially shorten the number of steps in organic synthesis. The complex, polycyclic, or highly functionalized structures can be obtained from simple substrates. New products that are challenging in synthesis using ground-state reactions are thus available, opening new perspectives in search of biologically active compounds.

The photochemical [2+2] cycloaddition reaction of alkenes with carbonyl compounds, referred to as the Paternò–Büchi (PB) reaction, was first reported in 1909 and is currently one of the versatile methods for oxetane synthesis (Scheme 1). Recent interest in this heterocycle is partly due to its biological activity. Oxetane rings have gained significant attention in medicinal chemistry as they can replace the gem-dimethyl and carbonyl groups to increase the "druglike" properties of a compound, especially its water solubility. Several biologically active oxetane-containing compounds have been found in nature, including 7-epi-10-deacetyltaxol with anticancer activity, norfriedelin A with acetylcholinesterase inhibitor activity, and macrolactins with antimicrobial activity.

Scheme 1 General mechanism of Paternò–Büchi reaction
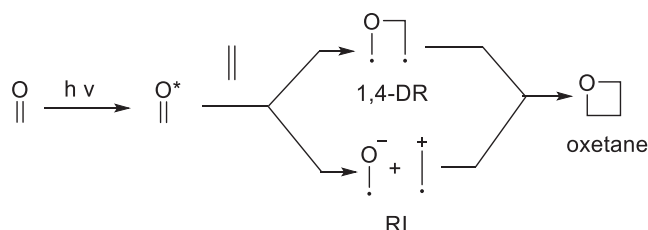
Danishefsky and Kitahara developed an acyclic siloxydiene, *trans*-1-methoxy-3-trimethylsilyloxy-buta-1,3-diene (*trans*-**1**). It is also known as the Danishefsky diene and is an useful reagent in organic synthesis. Since the diene is an electron-rich nucleophile, it proved to

be a powerful reagent in the Mukaiyama aldol addition and Diels-Alder reactions. For example, the reaction of benzaldehyde (**2a**) with *trans*-**1** at −78 °C in propionitrile solvent in the presence of 20 mol% acid catalyst afforded mainly the Mukaiyama aldol product **3** (Scheme 2). The C1 carbon of *trans*-**1** is the most nucleophilic centre, and thus, reacts with the electrophilic carbonyl carbon of **2a** to give the final 1,3 ketol product **3**. The hetero Diels-Alder reaction of **2a** with *trans*-**1** using a chiral zirconium catalyst gave the pyranone product 4 in 35% yield and 62% ee selectivity (Scheme 2).

In this study, the PB reaction of *trans*-**1** with benzophenone (**2b**) was examined for the first time, in which the formation of oxetanes **5** and **7** were found in high yields. So far, the PB reaction of acyclic conjugated dienes has not been studied. This is because the dienes are well-known to physically, rather than chemically, quench the triplet state of ketones, owing to their low triplet energy, E_T (~ 55 kcal mol^{-1}). The photochemically activated carbonyl compound reacted with *trans*-**1** to produce the C–C coupling compounds coupled at C2 and C3 carbon atoms, rather than C1 carbon atom. The chemoselectivities of the former are different from the Lewis acid-promoted reaction, indicating the synthetic utility of excited state.

Scheme 2 Mukaiyama aldol addition reaction, hetero Diels Alder reaction, and photochemical PB reaction of Danishefsky diene with carbonyl compounds

66

Acknowledgement

List of publications

List of Publications

(1) Photochemical [2+2] Cycloaddition Reaction of Carbonyl Compounds with Danishefsky
Diene

Dian Agung Pangaribowo and Manabu Abe

Organic & Biomolecular Chemistry, 18(26) (2020) 4962-4970.